Laser Produced Plasma Light Source for EUVL

Igor V. Fomenkov*, Alex I. Ershov, William N. Partlo, David W. Myers, Daniel Brown
Richard L. Sandstrom, Bruno La Fontaine, Alexander N. Bykanov, Georgiy O. Vaschenko
Oleh V. Khodykin, Norbert R. Böwering, Palash Das, Vladimir B. Fleurov, Kevin Zhang
Shailendra N. Srivastava, Imtiaz Ahmad, Chirag Rajyaguru, Silvia De Dea, Richard R. Hou
Wayne J. Dunstan, Peter Baumgart, Toshi Ishihara, Rod D. Simmons
Robert N. Jacques, Robert A. Bergstedt, David C. Brandt

Cymer Inc., 17075 Thornmint Court, San Diego, CA 92127, USA

ABSTRACT

This paper describes the development of laser-produced-plasma (LPP) extreme-ultraviolet (EUV) source architecture for advanced lithography applications in high volume manufacturing. EUV lithography is expected to succeed 193 nm immersion technology for sub-22 nm critical layer patterning. In this paper we discuss the most recent results from high qualification testing of sources in production. Subsystem performance will be shown including collector protection, out-of-band (OOB) radiation measurements, and intermediate-focus (IF) protection as well as experience in system use. This presentation reviews the experimental results obtained on systems with a focus on the topics most critical for an HVM source.

Keywords: EUV source, EUV lithography, Laser Produced Plasma

1. INTRODUCTION

EUV Lithography is the front runner for next generation critical dimension imaging after 193 nm immersion lithography for layer patterning below the 32 nm node; beginning in 2013 according to the International Technology Roadmap for Semiconductors (ITRS). NAND Flash and DRAM devices are expected to have the need for this manufacturing technology as soon as 2012, with pilot line system introduction starting this year (2011). The availability of high power 13.5 nm sources has been categorized as high risk and ranked as critical with other technologies requiring significant developments to enable the realization of EUV lithography. High sensitivity photoresists with good line-edge-roughness (LER) and line-width-roughness (LWR) are needed to keep the required source power within reasonable limits. Photoresist sensitivity and other light absorbing elements are the basis to derive EUV source power requirements within the usable bandwidth (BW) of 2 %. Scanner manufacturers are requiring clean EUV power of 250 W at the intermediate focus (IF) to enable > 100 wph scanner throughput assuming 15 mJ/cm^2 photoresist sensitivity. The need for a Spectral Purity Filter (SPF) increases the requirements for Raw EUV power even higher. Clean EUV Power is calculated by taking the Raw EUV power and subtracting the losses associated with the SPF and dose control.; For the current sources these losses are estimated to be 35% and 20%, respectively. A scalable EUV source architecture is needed to enable the evolution of EUV lithography during the life cycle of the technology. Laser-produced-plasma (LPP) sources are expected to deliver the necessary high power for critical-dimension high-volume manufacturing (HVM) scanners for the production of integrated circuits in the post-193 nm immersion era.[1,2]

A schematic of a source vessel is shown in Figure 1. An HVM I source is shown in Figure 2. Eight sources have been built and are operational, four of these have been shipped to customers. As described in details previously[3-5], the HVM I sources use a 5 sr normal incidence collector, tin droplets of 30 microns diameter, and a ~30 kW (average power) CO_2 laser. The HVM I source is shown in its inclined position of 27 degrees as it is positioned when integrated into the scanner.

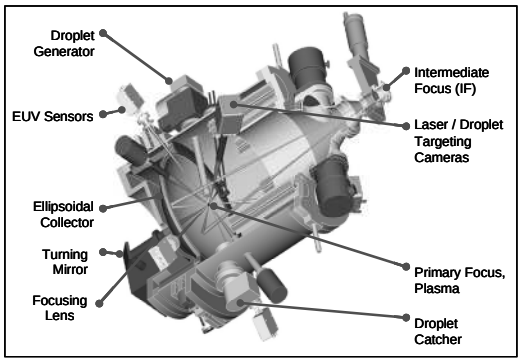

Figure 1: Schematic of source vessel

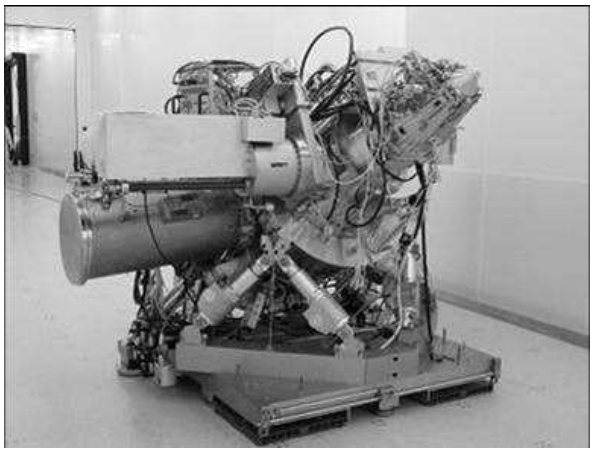

Figure 2: HVM I source vessel as shipped

2. SOURCE CHARACTERIZATION TOOL

A tool for qualification of the LPP sources was developed. The Far Field Test Tool (FFTT) is positioned behind IF and receives the light that would go onto the illumination optics if it were attached to a scanner. The FFTT provides capability of measurement of many parameters of the source.; This paper describes only few of them: the far field collector imaging, out-of-band measurements, and capabilities of the IF Protection module to suppress contamination.

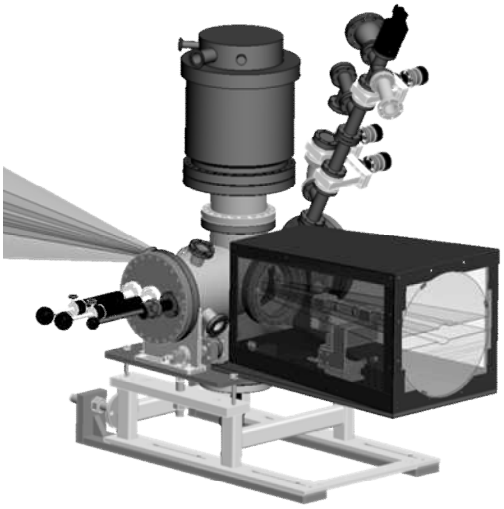

Figure 3: Far Field Test Tool (FFTT)

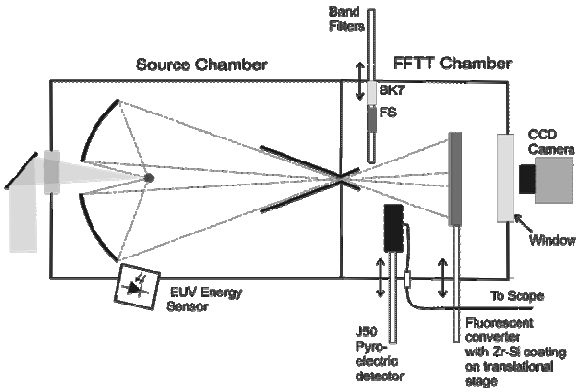

Figure 4: : FFTT Schematic

3. COLLECTOR QUALIFICATION

Cymer's LPP EUV source employs near-normal-incidence mirrors with a large solid angle for light collection. Such a geometry has numerous advantages, which has been discussed elsewhere.[6] As we reported earlier[1], the complete infrastructure is in place for manufacturing of large-size normal-incidence collector mirrors. For demonstration of the light collection capabilities of our source several 1.6 sr sub-

aperture versions (300 mm optical diameter) have been produced and used in the development system for testing. Full size (650 mm diameter) collectors with 5 sr collecting angle were fabricated for HVM I tools. The collectors have been coated with graded multilayer coatings with layer periods optimized for high EUV reflectance at the corresponding incidence angles.

A collector was installed into a HVM I source and run under operating conditions of 11W average exposure power (21 mJ dose controlled operation) for 90 hours. The quality of the collector protection was monitored during this long duration run with the FFTT taking an image every hour.

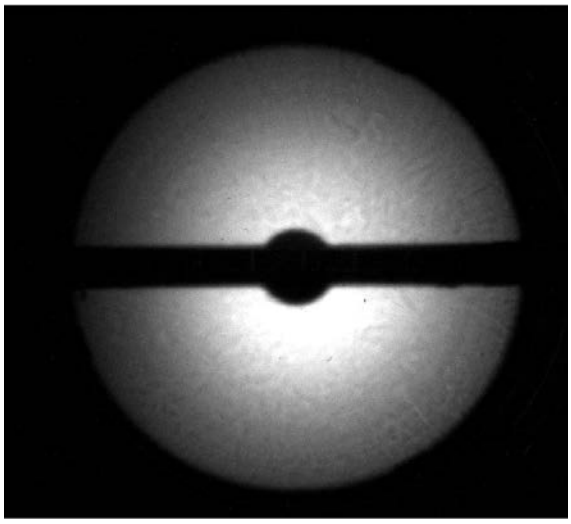

Figure 5: Initial far field image of the collector past IF (very few pulses)

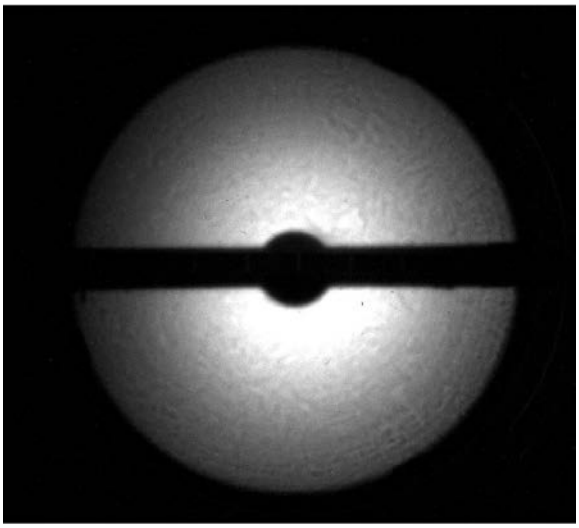

Figure 6: Far field image of the collector past IF after 6 billion pulses / 90 hours

The evolution of relative reflectivity versus exposure dose from this test is shown in a companion paper of these proceedings[7]. Before this test additional improvements in the gas flow distribution which is used for debris mitigation and multilayer coating have been implemented and resulted in no measurable loss of EUV reflectivity. This is evident by no visible change in EUV image after 6B pulses as shown in Figures 5 and 6. Further improvement in flow arrangement, vacuum environment cleanliness and multilayer coating are expected to provide continuous advancements throughout 2011 to allow the device makers to use the sources with less downtime associated with changing of the collector.

4. OUT-OF-BAND MEASUREMENTS

This section describes the development of a tool for OOB radiation measurements and discusses the measurements taken on Sn targets with a CO_2 laser. The tool uses three different fiber optics spectrometers with calibrated intensity from both solar spectrum and deuterium light source. A MatLab code was developed to apply the calibration curve to the radiation measured from plasma and presents the absolute intensities of the measured spectra in J/nm (into 2π solid angle) versus wavelength in nm for the spectral range from 200 to 950 nm. The exponential extrapolation of the measured spectral densities into the short and long wavelength ranges enables us to estimate the OOB radiation for the bands from 130 to 350 nm and from 1 to 5 μm, which are most critical for the EUV source application. Measurements with three spectrometers optimized for different bands revealed perfect stitching of the measurements in overlapped bands.

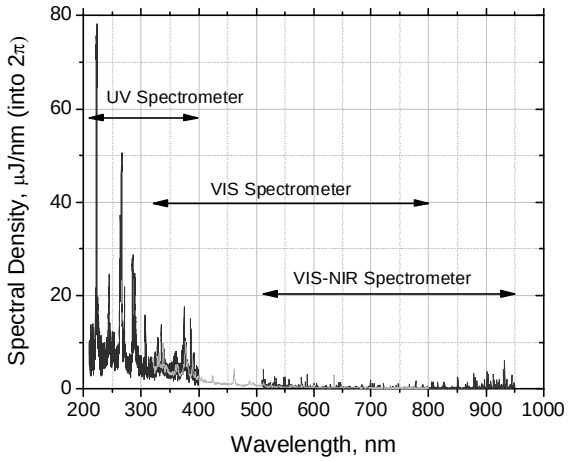

Figure 7: CO_2 laser / Sn droplet plasma OOB spectrum as measured with three different spectrometers

The requirements for OOB radiation are dictated by the requirements for high contrast patterning for a given photo-resist. Thus, several aspects of the process should be considered when determining the critical wavelength bands and critical radiation dose in these bands which are acceptable for the EUV tool. One aspect is the spectral sensitivity of the photo-resist. Another aspect is reflectivity of MLM collector for OOB radiation. OOB measurements taken with fiber optics spectrometers were calibrated by energy measurements with band filters on HVM I tools. The FFTT provides good measurement accuracy for the radiation energy within a given wavelength band-pass. Fused-Silica (FS) and Borosilicate glass (BK7) filters were used in the FFTT to take the measurements shown in Table 1. Most important is the energy difference from the measurements of these two filters, which provides a good indication of the energy that may expose a 193 nm based resist. The measurements show that only 1% of the in-band EUV radiation is in the wavelength range from 200 to 310 nm.

Band	**Measurement results**
EUV OOB, 10-35nm	FWHM calculated for reflectivity curve
DUV, 35-115nm	All radiation Absorbed by H2
UV+Visible+NIR, 200nm-3mm, (FS filter)	6-8% of In-Band EUV
UV, 200-310nm, (FS-BK7)	~1% of In-Band EUV

Table 1: Summary of out-of-band measurement results

5. IF PROTECTION

The IF Protection Module works on the basis of a dynamic gas lock with differential pumping. The FFTT provides a method to quantify the suppression of a surrogate contaminate (Ar) introduced into the source vessel side and measured on the FFTT side used an RGA. The measurement results shown provide three curves for three different pressures inside the FFTT vacuum chamber. A known quantity of Ar was injected into the source vessel, a differentially pumped RGA was used after IF for characterization of the gas lock. Initially differentially pumped RGA was calibrated with known partial pressure of Ar behind IF.. The ultimate suppression of Ar with full flow of the DGL is greater than the measurement capability of differentially pumped RGA. Extrapolating the suppression values for higher flow rates suggest capabilities well above the requirements.

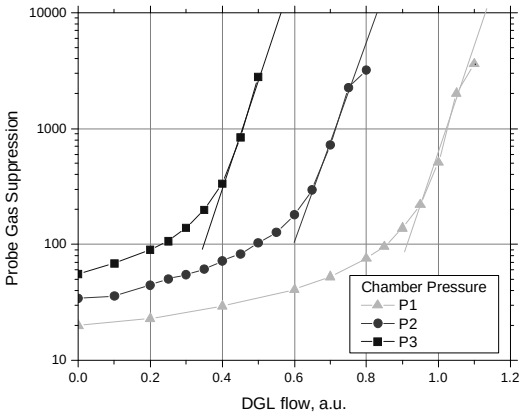

Figure 8: Contamination suppression vs. flow across the IF Protection Module

The IF Protection module not only provides suppression of contaminations which might migrate from the EUV source chamber into the vacuum space of the illumination optics, it also serves as an interface between the source and the scanner. Significant development by both Cymer and ASML have gone into the design of this module. It is now complete and has been adopted by ASML as the standard interface for EUV Scanners.

6. SUMMARY

Laser-produced plasma has been shown to be the leading source technology with scalability to meet requirements from leading scanner manufacturers and provide a path towards higher power as the lithography tools evolve over their life cycle. Normal-incidence collector mirrors of diameter > 650 mm, with > 5 sr light collection and average reflectivities >50% are produced and integrated into production LPP systems. The developed technique for debris mitigation proved stable operation of the collector without measureable degradation for at least 6B pulses which corresponds to the dose of about 4000 kJ. Measured out of band radiation from the source behind IF in visible and DUV bands meets industrial requirements dictated by high contrast patterning for the photo-resist. The IF Protection module demonstrates high suppression of possible contaminates from the EUV source for safe operation of the illuminator optics.

Eight HVM I LPP EUV source systems have been built and are operational, four of these sources have been shipped to customers. EUV lithography is expected to be the critical dimension imaging solution in the post-193 nm immersion era. LPP source technology with power levels exceeding 400W is expected to enable the IF power requirement projected in the future, and to provide the much needed margin for photoresist sensitivity, spectral purity filters, optics degradation, process latitude, and overall equipment throughput. Cymer is developing second generation (HVM II) EUV light sources in 2011. The company continues to meet its EUV source development commitments to industry, customers and suppliers.

ACKNOWLEDGEMENTS

The authors gratefully acknowledge the valuable contributions from Bob Lofgren, John Sporre and David N. Ruzic of University of Illinois, Urbana Champaign, Marco Perske, Hagen Pauer, Mark Schürmann, Sergiy Yulin, Torsten Feigl and Norbert Kaiser of Fraunhofer Institut f. Angewandte Optik und Feinmechanik, Eric Gullikson and Farhad Salmassi of Lawrence Berkeley National Laboratory, Frank Scholze, Christian Laubis, Christian Buchholz and coworkers at PTB, and Mark Tillack and Yezheng Tao of the University of California at San Diego. We are also very thankful for the invaluable support and

contributions, past and present, of many scientists, engineers and technicians involved in the EUV technology program at Cymer.

REFERENCES

[1] Fomenkov, I.V., Brandt, D.C., Bykanov, A.N., Ershov, A.I., Partlo, W.N., Myers, D.W., Böwering, N.R., Vaschenko, G.O., Khodykin, O.V., Hoffman, J.R., Vargas E.L., Simmons, R.D., Chavez, J.A., Chrobak, C.P., in: *Proc. of SPIE Vol. **6517**, Emerging Lithographic Technologies XI*, M. J. Lercel, ED., 65173J (2007).

[2] Brandt, D.C., Fomenkov, I.V., Ershov, A.I., Partlo, W.N., Myers, D.W., Böwering, N.R., Bykanov, A.N., Vaschenko, G.O., Khodykin, O.V., Hoffmann, J. R., Vargas E.L., Simmons, R.D., Chavez, J.A., Chrobak, C.P., in: *Proc. of SPIE Vol. **6517**, Emerging Lithographic Technologies XI*, M. J. Lercel, ED., 65170Q (2007).

[3] Brandt, D.C., Fomenkov, I.V., Ershov, A.I., Partlo, W.N., Myers, D.W., Böwering, N.R., Farrar, N.R., Vaschenko, G.O., Khodykin, O.V., Bykanov, A.N., Hoffman, J.R., Chrobak, C.P., Srivastava, S.N., Ahmad, I., Rajyaguru, C., Golich, D.J., Vidusek, D.A., De Dea, S., Hou, R.R., in: *Proc. of SPIE Vol. **7271**, Alternative Lithographic Technologies*, F. M. Schellenberg, B. M. La Fontaine, Eds., 727103, (2009).

[4] Fomenkov, I.V., Brandt, D.C., Bykanov, A.N., Ershov, A.I., Partlo, W.N., Myers, D.W., Böwering, N.R., Farrar, N.R., Vaschenko, G.O., Khodykin, O.V., Hoffman, J.R., Chrobak, C.P., Srivastava, S.N., Golich, D.J., Vidusek, D.A., De Dea, S., Hou, R.R., in: *Proc. of SPIE Vol. **7271**, Alternative Lithographic Technologies*, F. M. Schellenberg, B. M. La Fontaine, Eds., 727138 (2009).

[5] Böwering, N.R., Fomenkov, I.V., Brandt, D.C., Bykanov, A.N., Ershov, A.I., Partlo, W.N., Myers, D.W., Farrar, N.R., Vaschenko, G.O., Khodykin, O.V., Hoffman, J.R., Chrobak, C.P., Srivastava, S.N., Ahmad, I., Rajyaguru, C., Golich, D.J., Vidusek, D.A., De Dea, S., Hou, R.R., Journal of Micro/Nanolith. MEMS MOEMS 8(4), 041504 (2009).

[6] Böwering, N.R., Ershov, A.I., Marx, W.F., Khodykin, O.V., Hansson, B.A.M., Partlo, W.N., Vargas E. L., Chavez, J.A., Fomenkov, I.V., Myers, D.W., Brandt, D.C., in: *Proc. of SPIE Vol. **6151**, Emerging Lithographic Technologies X*, M. J. Lercel, Ed., 61513R (2006).

[7] Brandt, D.C., Fomenkov, I.V., Ershov, A.I., Partlo, W.N., Myers, D.W., Sandstrom, R.L., La Fontaine, B., Lercel, M. J., Bykanov, A.N., Böwering, N.R., Vaschenko, G.O., Khodykin, O.V., Srivastava, S.N., Ahmad, I., Rajyaguru, C., Das, P., Fleurov, V.B., Zhang, K., Golich, D.J., De Dea, S., Hou, R.R., Dunstan, W.J., Wittak, C.J., Baumgart, P., Ishihara, T., Simmons, R.D., Jacques, R.N., Bergstedt R.A., in: *these proceedings*, Proc. of SPIE Vol. **7969**, paper 51 (2011).

LPP Source System Development for HVM

David C. Brandt*, Igor V. Fomenkov, Alex I. Ershov, William N. Partlo, David W. Myers
Richard L. Sandstrom, Bruno La Fontaine, Michael J. Lercel, Alexander N. Bykanov, Norbert R. Böwering,
Georgiy O. Vaschenko, Oleh V. Khodykin, Shailendra N. Srivastava, Imtiaz Ahmad, Chirag Rajyaguru,
Palash Das, Vladimir B. Fleurov, Kevin Zhang, Daniel J. Golich, Silvia De Dea, Richard R. Hou, Wayne J. Dunstan
Christian J. Wittak, Peter Baumgart, Toshi Ishihara, Rod D. Simmons, Robert N. Jacques, Robert A. Bergstedt

Cymer Inc., 17075 Thornmint Court, San Diego, CA 92127, USA

ABSTRACT

Laser produced plasma (LPP) systems have been developed as a viable approach for the EUV scanner light sources to support optical imaging of circuit features at sub-22nm nodes on the ITRS roadmap. This paper provides a review of development progress and productization status for LPP extreme-ultra-violet (EUV) sources with performance goals targeted to meet specific requirements from leading scanner manufacturers. The status of first generation High Volume Manufacturing (HVM) sources in production and at a leading semiconductor device manufacturer is discussed. The EUV power at intermediate focus is discussed and the lastest data are presented. An electricity consumption model is described, and our current product roadmap is shown.

Keywords: EUV source, EUV lithography, Laser Produced Plasma

1. INTRODUCTION

EUV Lithography is the front runner for next generation critical dimension imaging after 193 nm immersion lithography for layer patterning below the 22 nm node; beginning in 2013 according to the International Technology Roadmap for Semiconductors (ITRS). NAND Flash and DRAM devices are expected to have the need for this manufacturing technology as soon as 2012, with pilot line system introduction starting this year (2011). The availability of high power 13.5 nm sources has been categorized as high risk and ranked as critical with other technologies requiring significant developments to enable the realization of EUV lithography. High sensitivity photoresists with good line-edge-roughness (LER) and line-width-roughness (LWR) are needed to keep the required source power within reasonable limits. Photoresist sensitivity and overall optical transmission through the EUV scanner are the basis to derive EUV source power requirements within the usable bandwidth (BW) of 2 %. Scanner manufacturers are requiring clean EUV power of 250W at the intermediate focus (IF) to enable > 100 wph scanner throughput assuming a photoresist sensitivity of 15 mJ/cm^2. The need for an IR spectral purity filter (SPF) increases the requirements for raw EUV Power even further.

Clean EUV Power is calculated by taking the raw EUV power and subtracting the losses associated with the spectral purity filter (SPF) and the dose control overhead; for current HVM I sources these losses are estimated to be 35% and 20%, respectively. A scalable EUV source architecture is needed to enable the evolution of EUV lithography during the life cycle of the technology. Laser-produced-plasma (LPP) sources are expected to deliver the necessary power for critical-dimension high-volume manufacturing (HVM) scanners for the production of integrated circuits in the post-193 nm immersion lithography era.[1]

LPP EUV lithography light sources generate the required 13.5 nm radiation by focusing a 10.6 micron wavelength CO_2 laser beam onto tin (Sn) targets creating a highly ionized plasma with electron temperatures of several 10's of eV. EUV photons are radiated isotropically by these ions. Photons are collected with a temperature controlled graded multi-layer coated normal-incidence mirror (collector), and focused to an intermediate point from where they are relayed to the scanner optics and ultimately to the wafer. High conversion efficiency (CE) of the laser energy into EUV energy is critical to meeting the required power levels. The collector is protected from the plasma by a debris mitigation

technology based on a hydrogen buffer gas. High-energy ions, fast neutrals, and residual source element particles are mitigated to maintain the reflectivity of the collector mirror and enable a long lifetime of this component. Diagnostics measuring the properties of emitted light at both the plasma and IF are used to characterize the output of the source.[2] Performance results of test and prototype light sources obtained up to about a year ago have already been described in detail previously.[1,3,4,5]

2. LPP SOURCE SYSTEM

The system architecture is shown in a scale drawing in Figure 1. The three major subsystems of the source are the drive laser, the beam transport system (BTS) and the source vessel. The drive laser is a CO_2 laser with multiple stages of amplification to reach the required power level of up to ~30 kW.[1,6] It is operated in pulsed mode at ~50 kHz with radio-frequency (RF) pumping from generators (not shown) operating at 13.56 MHz. The laser is typically installed in the sub-fab along with its RF generators and water-to-water heat exchangers. The laser beam is expanded as it leaves the drive laser to lower the energy density on the BTS mirrors. Three turning mirrors are used to allow the beam to travel from the sub-fab to the fab through the waffle-slab floor with the needed flexibility for positioning the laser with respect to the source vessel (and scanner) on the floor above. The laser and BTS are completely enclosed and interlocked to meet laser class 1 requirements. The BTS delivers the beam to a focusing optic where the 10.6 micron wavelength light is focused to a minimum spot size defined by the numerical aperture of the focusing system. The focused beam propagates through a central aperture in the collector and strikes the droplet at the focus of the ellipsoidal collector mirror inside the vacuum space of the source vessel. The droplet generator delivers liquid tin droplets of 30 micron diameter to the same position at ~ 50 kHz repetition rate; both laser pulse and droplets are steered and timed to ensure proper targeting. The laser pulse vaporizes and heats the tin into a plasma cloud of critical temperature and density. The EUV light emitted by the plasma is collected and reflected with the multi-layer coated ellipsoidal mirror to the IF where it passes through a small aperture into the scanner volume that houses the illumination optics.

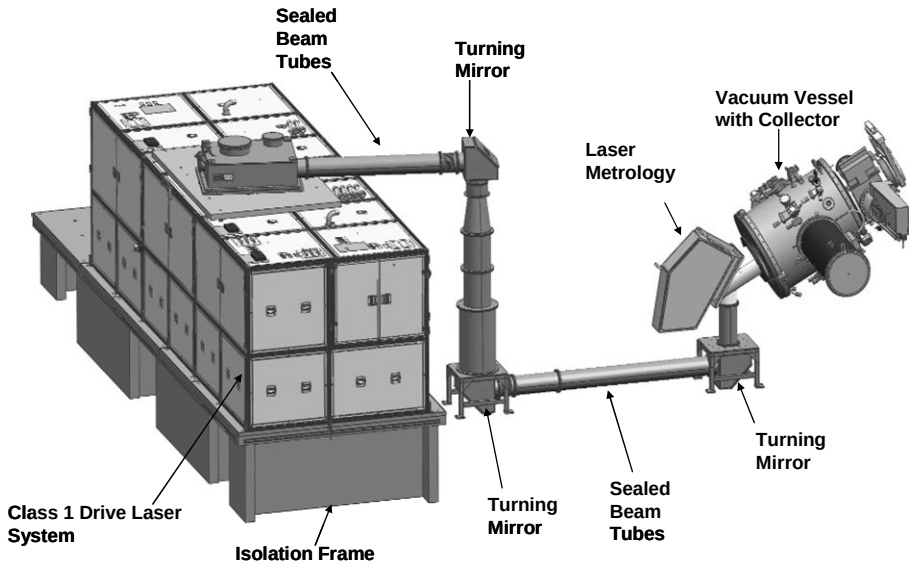

Figure 1: Scale Drawing of Laser Produced Plasma Source.

To ensure that no contamination can reach the scanner volume an IF protection module surrounds the aperture and suppresses flow or diffusion. Other modules on the source vessel include the droplet catcher which collects the unused droplets between the bursts, and metrology modules for measuring EUV energy and for imaging of droplets and plasma. The source controller turns on and off bursts of pulses as commanded by the scanner, which can be as long as several seconds. Exposures at full source power correspond to typically several hundred milliseconds for a 26 x 33mm field size

using 15 to 20mJ/cm^2 resist. The ratio of time when the burst is on to the period between bursts defines the intra-field duty cycle.

Eight first-generation HVM I sources have been completed and are operational. Four of these sources have been installed at customers, including one at a leading semiconductor device maker R&D facility. An HVM I source vessel is shown in Figure 2 positioned at the specified source orientation angle. Figure 3 shows this source vessel integrated into the NXE 3100 scanner and fully enclosed inside the body of the system.

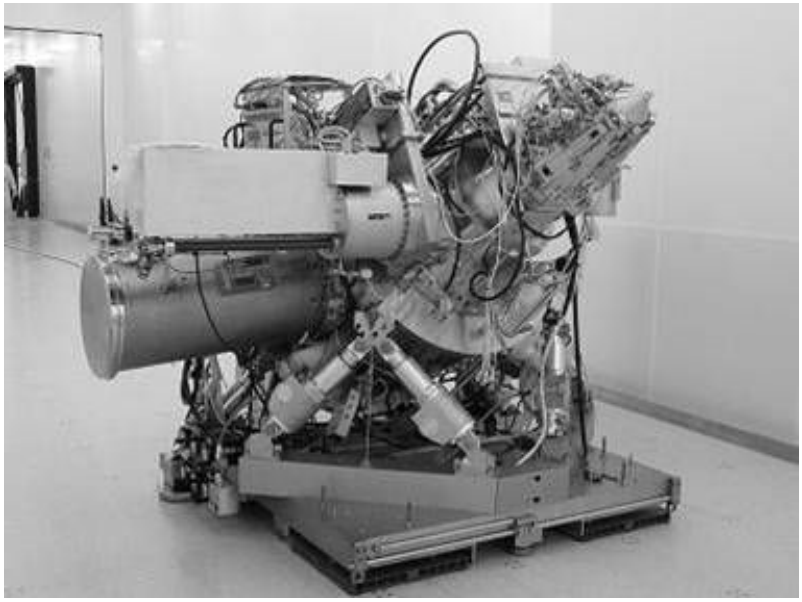

Figure 2: HVM I LPP Source Vessel moving into the customer clean room.

Figure 3: HVM I LPP Source Vessel Integrated into the NXE 3100 Scanner.

3. RECENT DEVELOPMENT RESULTS

Figure 4 shows the dose controlled EUV energy per burst measured on an HVM I source running at ~50% duty cycle, as determined from measurements at plasma. The usable average exposure power is ~11W, as calculated using the assumptions of 5sr solid angle, 50% collector reflectivity, 90% gas and 65% SPF transmission. The feasibility of dose stability meeting the final production requirement of <±0.20% 3σ has been demonstrated, as can be seen in Figures 4 and 5. The data shown is within wafer in Figure 4 and within exposure field in Figure 5. The processing of the data in this way is possible because the source was being driven in a scanner simulation mode during these exposures to replicate the on/off cycling from exposing fields and waiting for the scanner to move to the next field. .

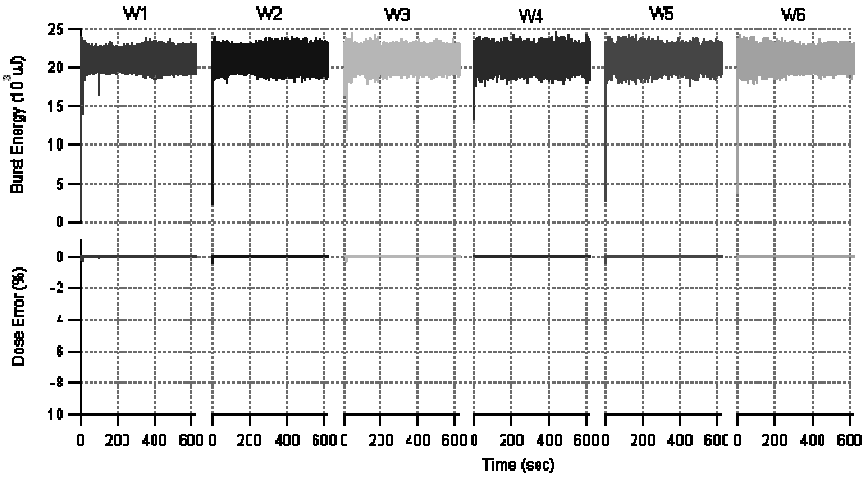

Figure 4: Dose controlled EUV energy within wafer (upper chart), 6 wafers: Dose stability within wafer (lower chart)

This scanner simulator is a control system emulating a real scanner in a control rack interfaced with our source during testing while the sources are in San Diego. These experiments were performed using tin droplets with 30 micron diameter at 40kHz repetition rate and a nominal 5 seconds per exposure field on one of our HVM I sources. This level of performance will provide a throughput of approximately 6 wafers per hour on an NXE 3100 scanner when using a photoresist sensitivity of 10mJ/cm^2

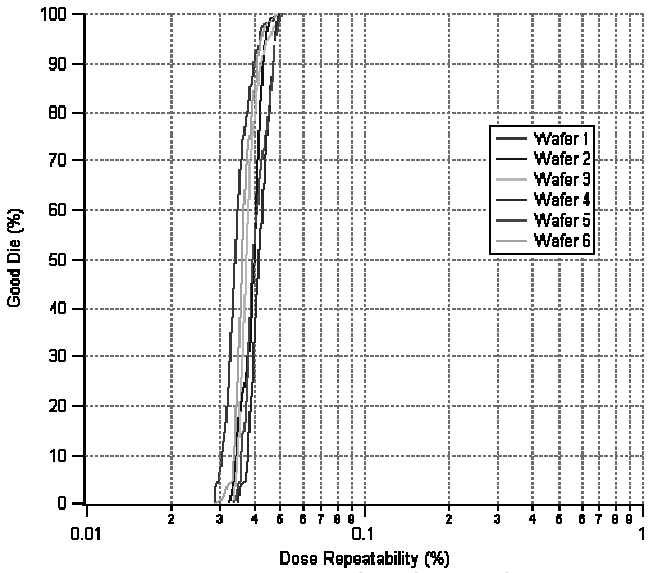

Figure 5: Dose stability distribution within exposure field for 6 wafers

The average area-weighted EUV reflectivity of ten new collectors was measured to be up to 52.1%, see Figure 6 for reflectance results. Several long duration tests have been performed to evaluate the collector protection capability of HVM I sources. Relative reflectivity is monitored using the FFTT during testing to evaluate the efficiency of protection, the difference between the first two data sets (Sept 2010 vs. Feb 2011) demonstrates new gas flow balancing techniques over 50 hours duration , as shown in Figure 7, as was described in the talk at Advanced Lithography.

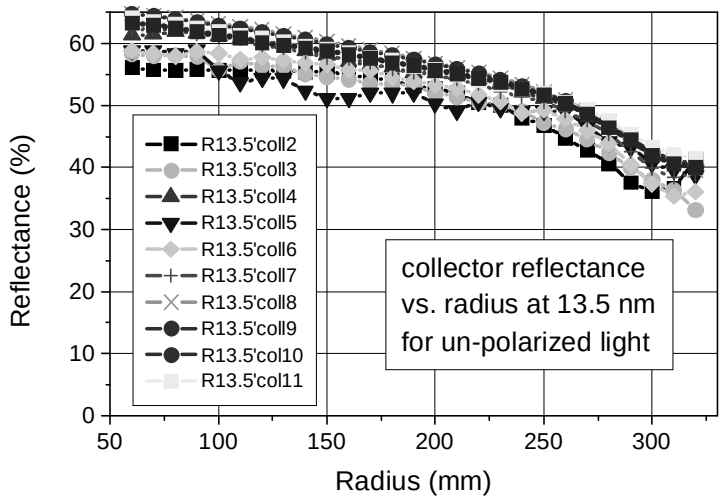

Figure 6: EUV Reflectivity of new Collectors vs. Mirror Radius as measured on a beam line at PTB

Also shown in Figure 7 are more recent results from a 90 hours test using improvements to the coating technology as discussed in the talk. The March 2011 results indicate no degradation of relative reflectivity while delivering a dose of >4MJ to the IF. 4MJ corresponds to approximately 512 wafers or 5.7 wafers per hour assuming 10mJ/cm^2 resist sensitivity and current assumptions for SPF and scanner transmission. Relative average reflectivity vs. exposure dose at IF is plotted in the graph. The data from September 2010 (open squares) was taken during operation at a nominal 6W of average EUV exposure power, while the data from February 2011 (open circles) was taken during operation at 11W power.

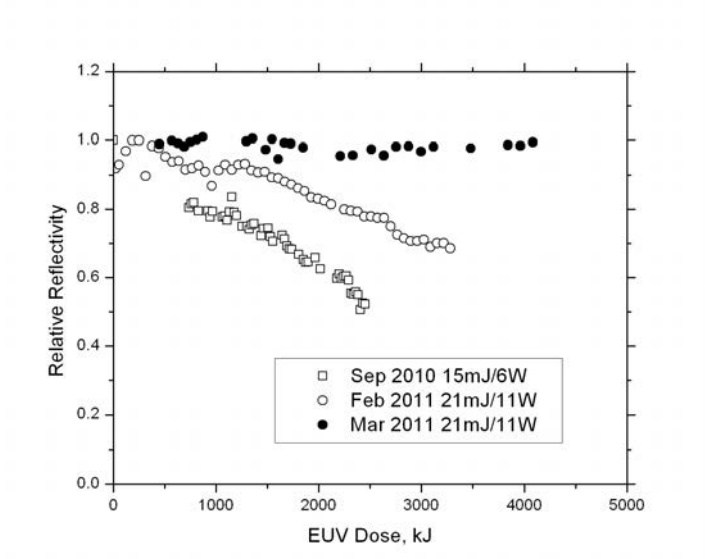

Figure 7: Relative Reflectivity measured during Exposure for three different tests

The newer data (dark circles) shows a significantly reduced reflectivity loss during exposure and is a result of improvements made in the overall protection for the multilayer coating on the surface of the normal-incidence collector. Further improvements are planned to be implemented during 2011 in the areas of gas flow uniformity, vacuum environment cleanliness and multilayer coatings to enable the source to provide an expected collector lifetime of several months and ultimately one year.

Development of our pre-pulse sub-system was completed on our LT1 source for research and development[7]. The pre-pulse expands the droplet target to a larger size and lowers the density before the main pulse irradiates it at the primary focus of the collector. The raw EUV power produced using pre-pulse on LT1 was approximately 160W during operation at 40kHz repetition rate, as shown in Figure 8. The data was collected at low duty cycle (~3%) with no dose control.

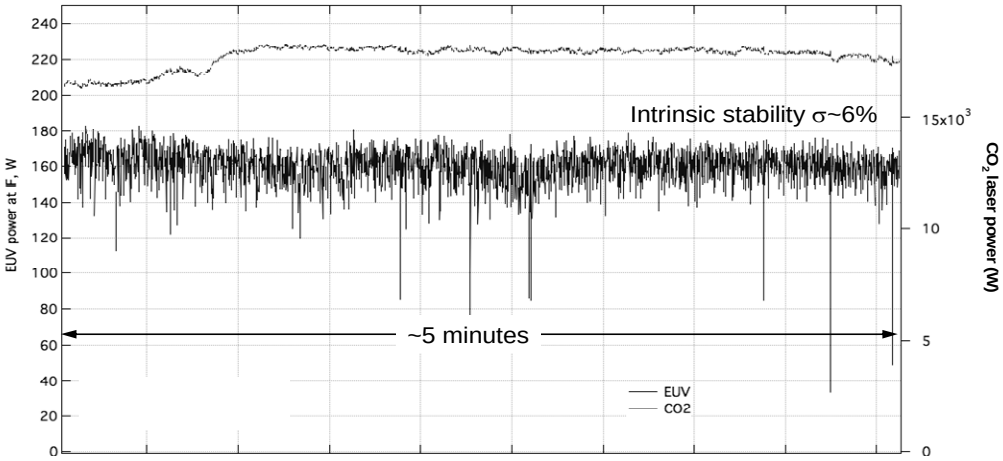

Figure 8: Pre-Pulse Operation on LT1

The CO_2 laser power was approximately 17.5 kW as shown by the second line on the graph in figure 8, corresponding to roughly 3% conversion efficiency (CE), as shown in Figure 9. The pre-pulse sub-system is currently integrated onto an HVM I source in San Diego and being tested in order to determine the optimum operating conditions and maximum usable power when running under high duty cycle and dose-controlled conditions.

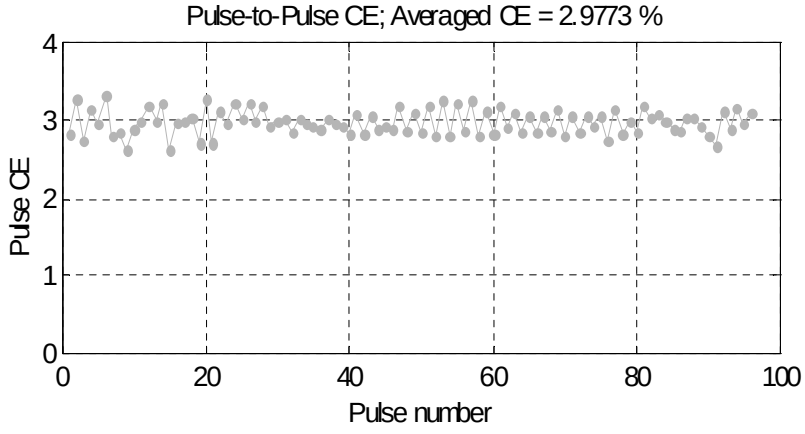

Figure 9: Pulse-to-Pulse Conversion Efficiency

Each of the eight HVM I sources is planned to be upgraded with the pre-pulse subsystem in the fourth quarter of 2011. The sources as shipped have reserved space for this additional hardware to fit within the existing footprint of the drive laser. With this upgraded configuration the HVM I sources are expected to provide the final specification for power output of 105W average exposure power.

4. ELECTRICITY CONSUMPTION

A major utility for the EUV source is the electrical power that the system requires. With the operation of the EUV source at nominal scanner operating conditions we can estimate with reasonable certainty the amount and cost of the electrical power used. These calculations are shown in Figure 10. The histogram for HVM II sources shows decreasing cost of electrical consumption due to higher efficiency of the solid-state RF generators planned to be used on these sources in addition to a lower overall use of a higher power EUV source. The percentage of burst on-time required for the exposure is decreased as the power of the source is increased, resulting in a lower usage of electrical consumption and a lower cost. It should be noted that the cost of electricity consumption used here was based on 0.09 $/kWhr. .

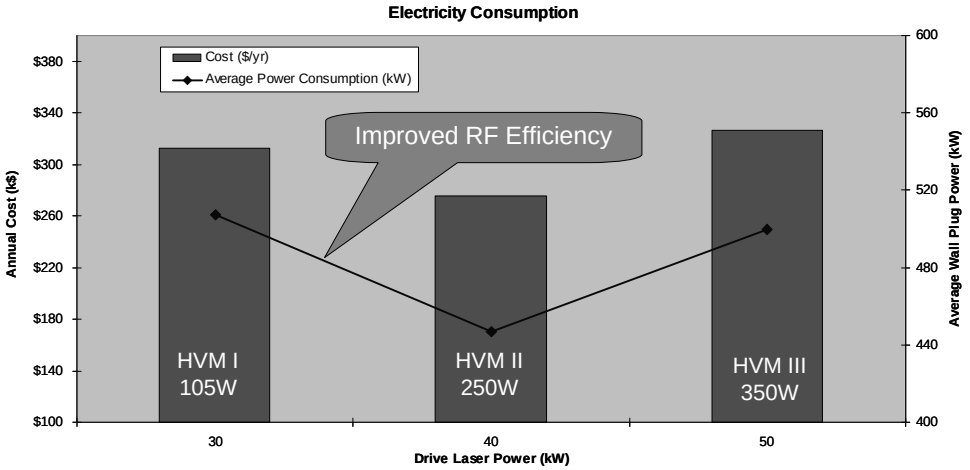

Figure 10: Estimated usage and cost of electrical power for EUV sources

5. ROADMAP

The LPP source roadmap is shown in Figure 11. The HVM I product is expected to meet requirements for pre-production or beta generation scanners in 2011 with clean EUV output powers of >100 W using a 30 kW CO_2 laser system on 30 micron diameter Sn droplets with 3.0 % CE. The normal-incidence collectors used have a collection solid angle of ~ 5 sr and multilayer coatings with EUV reflectivity > 50 % on average over the surface. Transmission losses due to gas absorption and debris mitigation techniques are projected to be less than 20 % and SPF losses are expected to be 35%. Scanner roadmap requirements for later generation LPP EUV sources will drive source powers to 350 W (HVM III) with CO_2 laser power delivering ~50 kW of power. Further improvements in CE and collection efficiency are expected to enable clean EUV power levels that meet these requirements.

EUV Source Power Roadmap			
Source Model	HVM I	HVM II	HVM III
Drive Laser Power (kW)	**30**	**40**	**50**
In-band CE (%)	3.0	3.5	4.0
Collection Efficiency (sr)	5	5.5	5.5
Collector Reflectivity (%)	50	50	50
Clean EUV Power (W)	**105**	**250**	**350**

Figure 11: Projected LPP EUV Source Roadmap

6. SUMMARY

Laser-produced plasmas have been shown to be the leading source technology with scalability to meet requirements from leading scanner manufacturers and provide a path toward higher power as the lithography tools evolve over their life cycle. An EUV power of 160W at intermediate focus at low duty cycle has been reported. The feasibility of meeting the dose stability target of <0.2% has been demonstrated. Normal-incidence collector mirrors of diameter > 650mm, with > 5 sr light collection and average reflectivity >50% are produced and integrated into production LPP systems. The combination of 10.6 μm laser light and Sn source element has demonstrated a CE in excess of 3 %. LPP source technology with power levels of 350W is expected to satisfy the IF power requirement projected in the future.

ACKNOWLEDGEMENTS

The authors gratefully acknowledge the valuable contributions from Bob Lofgren, John Sporre and David N. Ruzic of University of Illinois, Urbana Champaign, Marco Perske, Hagen Pauer, Mark Schürmann, Sergiy Yulin, Torsten Feigl and Norbert Kaiser of Fraunhofer Institut f. Angewandte Optik und Feinmechanik, Eric Gullikson and Farhad Salmassi of Lawrence Berkeley National Laboratory, Frank Scholze, Christian Laubis, Christian Buchholz and coworkers at PTB, and Mark Tillack and Yezheng Tao of the University of California at San Diego. We are also very thankful for the invaluable support and contributions, past and present, of many scientists, engineers and technicians involved in the EUV technology program at Cymer. We are also thankful to colleagues at ASML for helpful discussions of various aspects related to the light source operation.

REFERENCES

[1] Fomenkov, I.V., Brandt, D.C., Bykanov, A.N., Ershov, A.I., Partlo, W.N., Myers, D.W., Böwering, N.R., Vaschenko, G.O., Khodykin, O.V., Hoffman, J.R., Vargas, E., L., Simmons, R.D., Chavez, J.A., Chrobak, C.P., in: *Proc. of SPIE Vol. **6517**, Emerging Lithographic Technologies XI*, M. J. Lercel, ED., 65173J (2007).

[2] Böwering, N.R., Hoffman, J.R., Khodykin, O.V., Rettig, C.L., Hansson, B.A.M., Ershov, A.I., Fomenkov, I.V., in: *Proc. SPIE **Vol. 5752**, Metrology, Inspection, and Process Control for Microlithograpy XIX*, R. M. Silver, Ed., 1248-1256 (2005).

[3] Brandt, D.C., Fomenkov, I.V., Ershov, A.I., Partlo, W.N., Myers, D.W., Böwering, N.R., Farrar, N.R., Vaschenko, G.O., Khodykin, O.V., Bykanov, A.N., Hoffman, J.R., Chrobak, C.P, Srivastava, S.N., Ahmad, I., Rajyaguru, C., Golich, D.J., Vidusek, D.A., De Dea, S., Hou, R.R., in: *Proc. of SPIE Vol. **7271**, Alternative Lithographic Technologies*, F. M. Schellenberg, B. M. La Fontaine, Eds., 727103, (2009).

[4] Fomenkov, I.V., Brandt, D.C., Bykanov, A.N., Ershov, A.I., Partlo, W.N., Myers, D.W., Böwering, N.R., Farrar, N.R., Vaschenko, G.O., Khodykin, O.V., Hoffman, J.R., Chrobak, C.P., Srivastava, S.N., Golich, D.J., Vidusek, D.A., De Dea, S., Hou, R.R., in: *Proc. of SPIE Vol. **7271**, Alternative Lithographic Technologies*, F. M. Schellenberg, B. M. La Fontaine, Eds., 727138 (2009).

[5] Böwering, N.R., Fomenkov, I.V., Brandt, D.C., Bykanov, A.N., Ershov, A.I., Partlo, W.N., Myers, D.W., Farrar, N.R., Vaschenko, G.O., Khodykin, O.V., Hoffman, J.R., Chrobak, C.P., Srivastava, S.N., Ahmad, I., Rajyaguru, C., Golich, D.J., Vidusek, D.A., De Dea, S., Hou R.R.,, Journal of Micro/Nanolith. MEMS MOEMS 8(4), 041504 (2009).

[6] Fomenkov, I.V., Hansson, B.A.M., Böwering, N.R., Ershov, A.I., Partlo, W.N., Fleurov, V.B., Khodykin, O.V., Bykanov, A.N., Rettig, C.L., Hoffman, J.R., Vargas E.L., Chavez, J.A., Marx, W.F., Brandt, D.C., in: *Proc. of SPIE Vol. **6151**, Emerging Lithographic Technologies X*, M. J. Lercel, Ed., 61513X (2006).

[7] Brandt, D.C., Fomenkov, I.V., Ershov, A.I., Partlo, W.N., Myers, D.W., Böwering, N.R., Bykanov, A.N., Vaschenko, G.O., Khodykin, O.V., Hoffmann, J. R., Vargas E.L., Simmons, R.D., Chavez, J.A., Chrobak, C.P., in: *Proc. of SPIE Vol. **6517**, Emerging Lithographic Technologies XI*, M. J. Lercel, ED., 65170Q (2007).

Focus Drilling for Increased Process Latitude in High-NA Immersion Lithography

Ivan Lalovic, Jason Lee, Nakgeuon Seong, Nigel Farrar
Cymer, Inc., 17075 Thornmint Court, San Diego, CA 92127

Michiel Kupers*
Cymer B.V., De Run 4312-B, 5303 LN Veldhoven, The Netherlands

Hans van der Laan, Tom van der Hoeff, Carsten Kohler
ASML, De Run 6501, 5504 DR Veldhoven, The Netherlands

ABSTRACT:

In this paper we discuss a laser focus drilling technique which has recently been developed for advanced immersion lithography scanners to increase the depth of focus and therefore reduce process variability of contact-hole patterns. Focus drilling is enabled by operating the lithography light-source at an increased spectral bandwidth, and has been made possible by new actuators, metrology and control in advanced dual-chamber light-sources. We report wafer experimental and simulation results, which demonstrate a process window enhancement for targeted device patterns. The depth of focus can be increased by 50% or more in certain cases with only a modest reduction in exposure latitude, or contrast, at best focus. Given this tradeoff, the optimum laser focus drilling setting needs to be carefully selected to achieve the target depth of focus gain at an acceptable contrast, mask error factor and optical proximity behavior over the range of critical patterning geometries. In this paper, we also discuss metrology and control requirements for the light-source spectrum in focus drilling mode required for stable imaging and report initial trend monitoring results over several weeks on a production exposure tool. We additionally simulate the effects of higher-order chromatic aberration and show that cross-field and pattern-dependent image placement and critical dimension variation are minimally impacted for a range of focus drilling laser spectra. Finally, we demonstrate the practical process window benefits and tradeoffs required to select the target focus drilling laser bandwidth set-point and increase effectiveness of the source-mask solution for contact patterning.

Keywords: ArF immersion lithography, depth of focus, resolution enhancement, process latitude, excimer laser

I. INTRODUCTION

Double-patterning ArF immersion lithography continues to advance the patterning resolution and overlay requirements and has enabled the continuation of semiconductor bit-scaling. In order to pattern a range of 2D structures at the minimum resolution, high-NA lithography often results in process performance that is limited by the available depth of focus (DOF), particularly for patterning of contacts, vias or trenches. Achieving sufficient overlapping DOF over a range of geometries can be particularly challenging for these applications. This DOF constraint can lead to significant pattern variability, particularly when wafer topography and the overall focus budget is considered. Therefore, lithographers today employ a range of design, process and resolution enhancement techniques to overcome the depth of focus and other variability constraints required for manufacturability of sub-45 nm half-pitch technologies.

In this paper we present a method for increasing the DOF of contact or via patterns using the light-source, which is designed to minimize the reduction in exposure latitude. To illustrate this effect, Figure 1 shows the scanner aerial image-sensor measurement through focus as the laser spectral bandwidth (E95) is switched from a low to high setting, resulting in an observed increase in the depth of focus.

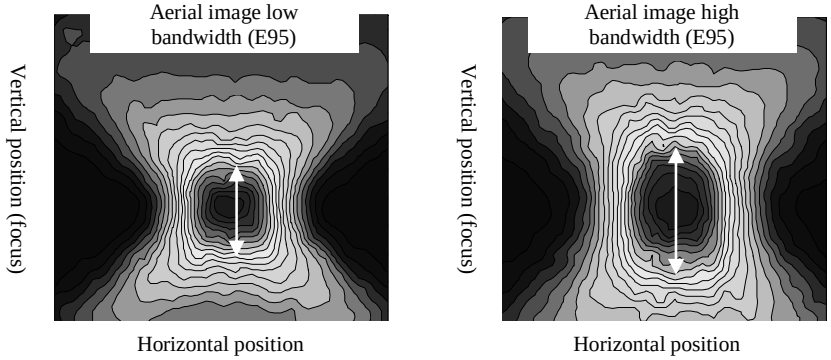

Figure 1. Image-sensor measurement of intensity through focus for low E95 (nominal) and high E95 (focus drilling)

* Currently at ASML, De Run 6501, 5504 DR Veldhoven, The Netherlands

Various methods of "drilling" through focus have been considered in the past in order to increase the lithographic depth of focus (DOF).[1,2] For example, in step-and-repeat systems the stage can be step-wise or continuously moved in the z-direction during field exposure, while in scan-and-repeat systems the stage (or image slit) can be tilted at a constant angle along the slit axis during exposure. An alternative method has been developed, as discussed in this work, which makes use of the changes in the laser bandwidth to enlarge the depth of focus. An advantage of this approach is that the wafer stage operation is not affected and scanning is performed with no additional movement in the z-direction, which is particularly beneficial for high-productivity immersion lithography.

1.1 Depth of Focus (DOF) Enhancement

An example aerial image response through-focus for a 32 nm logic technology contacts, obtained using a commercial lithography simulator, is shown in Figure 2 below for immersion 1.35NA soft-Quasar® illumination. Here the maximum image modulation, or maximum image contrast, occurs at a defocus of 0 nm and decays (quadratically) as the defocus increases.

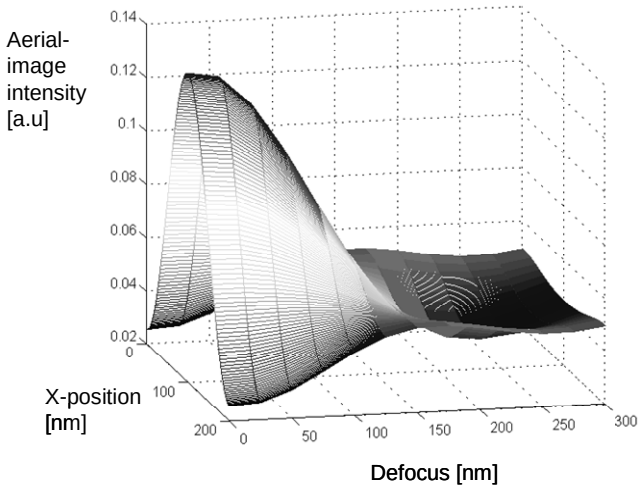

Figure 2. Example lithographic aerial image response through focus; 1.35NA ArFi

In this example the aerial image modulation at a 150nm defocus is minimal and a further increase in defocus results in image reversal, whereby an image minimum is observed at the location of the image maximum at best focus. Therefore in order to increase the image contrast out of focus, any focus drilling approach, must increase the intensity of the images for specific regions of defocus and minimize the contribution of images where image contrast is too low, or image reversal occurs. Since defocus is proportional to wavelength offset,[3,4] in lithographic exposure systems, this can be achieved using changes in the bandwidth of the light-source. The spectrum of the light-source will therefore have a significant impact on the exact amount of contrast enhancement out of focus. The specific choice of light-source actuators, and metrology described in this work is chosen to maximize the DOF enhancement and minimize the contrast reduction from spectral intensities in the low-contrast or image-reversal regions. The ability to control and stabilize light-source operation in the focus drilling mode is critical to ensure stable imaging performance (see reference 5 for more details).

1.2 Focus Drilling Application

The application of focus drilling is targeted for 2D dark-field patterns where the DOF is most constrained and also to enable a maximum process window overlap for multiple pattern geometries. Focus drilling would typically be applied to contact-hole, via or trench patterning. In addition to increasing the overlap process window, this approach may also provide additional degrees of freedom for an optimized OPC solution[7] and potentially relaxed mask requirements.

In the current implementation, laser focus drilling is activated from the scanner exposure recipe with a specific set-point and control value. This drives the light-source to operate and stabilize operation at the desired set-point bandwidth, which is entirely automated enabling equivalent system performance and stability as for nominal laser operation. No additional user interaction with the laser is required to enable focus drilling exposure.

1.3. Light-source Operation

Recent advancements in two-chamber master-oscillator power-amplifier (MoPa) light-sources have enabled new concepts for focus drilling implementation. Current approaches include the design of new actuation within existing line narrowing modules to enable fast and continuous spectral width adjustment and stabilization. The new

actuators are applied using existing optical elements, which results in enhanced light-source stability in both nominal and focus drilling modes.

Accurate light-source stabilization for focus drilling requires new advancements in spectrum metrology and compensation schemes which stabilize lithographic CD, dose-to-size, focus, process window and proximity behavior. New spectrum reconstruction approaches have enabled such advanced control schemes. The metrology and control requirements will be discussed further in this paper in the simulation and experimental results sections. The light-source technology required to enable the focus drilling actuation and spectrum metrology are described in more detail in reference 5.

II. SIMULATION RESULTS

2.1. Process Window (PW) Enhancement

Previously.[2,6,7] various researchers have shown that process window and particularly the depth of focus of 2D contact and via structures can be enhanced by broadening the laser bandwidth. These results have been obtained by simulation and confirmed experimentally for KrF and ArF (dry and immersion) lithography processes using various techniques to experimentally modify the light-source operation or perform multiple exposure passes. In Figure 3, below, we show a process window simulation result for 32nm logic contact / via pattern with 165nm pitch. In this case the ArF immersion numerical aperture is 1.35 with annular illumination.

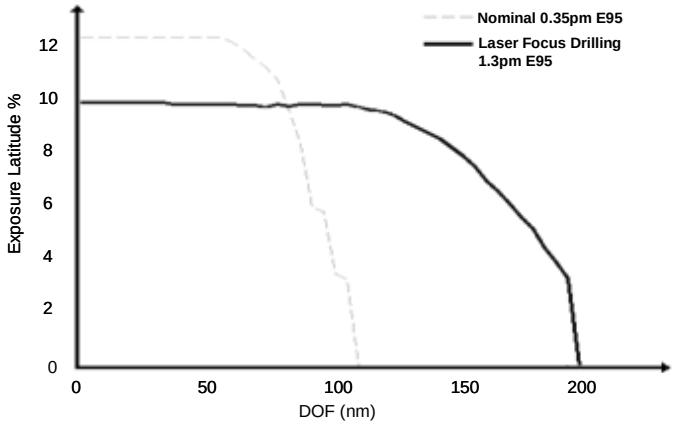

Figure 3. Process window for 1.35NA ArFi exposure for nominal light-source bandwidth (0.35pm E95) and a focus drilling spectrum (1.3pm E95)

For this simulated structure with pitch of 165nm a 60% - 70% DOF increase can be obtained using the Cymer Focus Drilling spectrum (at 1.3pm E95) over the nominal light-source operation (0.35pm E95) at best dose. In this paper, all of the simulations were carried out using Hyperlith or EM-Suite lithography simulation software from Panoramic Technology (http://www.panoramictech.com).

2.2 Focus Drilling Set-point Metrology and Control

The focus drilling set-point for the desired patterning application is selected by considering the overlap process window for all critical geometries that must be resolved simultaneously and defining the focus drilling level at which the required manufacturing focus margin can be met. At the same time the adverse impacts on exposure latitude (contrast loss), mask error factor and proximity effects must be characterized and managed. So far in this paper, we have described focus drilling spectral bandwidths in terms of the industry-standard E95 (95% energy integral) measurement,[8] which is available on board advanced dual-chamber light-sources for monitoring and closed-loop stabilization. This metric is a good predictor of the lithographic imaging performance for nominal light-source operation for control of critical dimension through focus, dose and mask bias.[9]

For the focus drilling application, spectral shape effects become increasingly important as the level of focus drilling increases, and bandwidths above 1pm E95 are required. In Figure 4, we show the CD simulation results for a 32nm logic process at 1.35NA with annular illumination (the corresponding process window for 165nm pitch is shown in Figure 3) for two groups of spectra at 1.2pm E95 obtained experimentally where the variation in spectral shape is maximized (Figure 4-a).

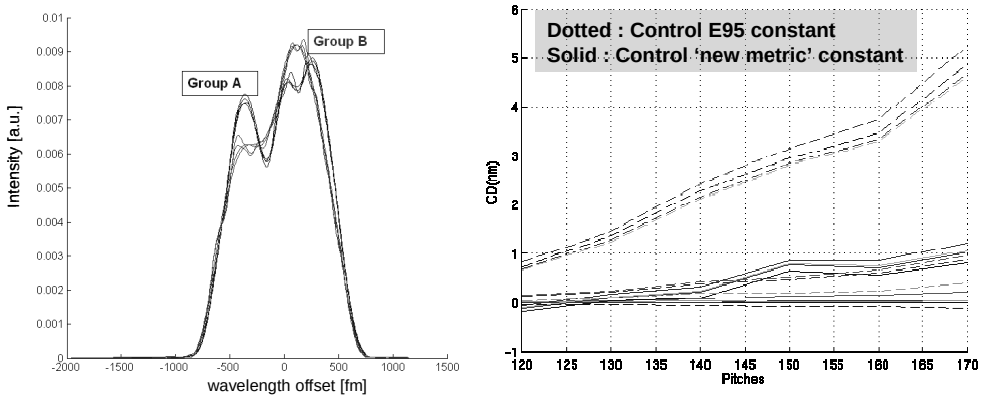

Figure 4. a) Range of experimentally obtained asymmetric spectral shapes, b) CD through pitch due to spectral shape change when spectra are re-scaled to 1.2pm E95 (dotted), or when re-scaled to keep a 'new metric' constant (solid)

For the focus drilling applications, with set-points > 1pm, spectral shape variation leads to changes in proximity effect, which need to be compensated in order to enable stable imaging performance. The bandwidth metrology on-board the light-source must enable full spectrum measurement in order to implement an accurate compensation scheme, as discussed in the next section. One such approach is demonstrated in Figure 4-b, where the dashed lines represent the CD change over the spectral variations shown in 4-a when the width of the spectra is held constant at 1.2pm E95, while the solid lines show the CD change with a new spectral metric constant. Control against this metrics reduces the lithographic variability to sub-1nm over a range of spectral shapes and through focus.

2.3. New bandwidth metric for laser Focus Drilling: Convolved Bandwidth (CBW)

A full-spectral-profile measurement capability has recently been developed that can be integrated with state-of-the-art light-sources for real-time spectral metrology. This is an enabling technology designed to meet the stringent CD control and stability requirements for immersion and double-patterning lithography applications for the focus drilling application. This technology and operational principles are discussed in reference 5. Given that accurate light-source spectral profiles can now be accessed during the operation of the light-source, a choice of metrics can be derived to robustly predict and enable closed-loop feedback for stable lithographic CD performance.

ASML and Cymer have introduced a new bandwidth metric that has very good correlation to the lithographic CD over broad variation in focus drilling spectral shapes and applies for set-points in excess of 1pm. This metric, termed convolved bandwidth (or CBW), is computed as a convolution of a proprietary function with the measured laser spectrum obtained on-board the laser and is used to compute real-time offsets for closed-loop control. An example correlation of the CBW metric to lithographic CD is shown in Figure 5 over a range of spectral shape variation for the 32nm logic imaging condition discussed previously.

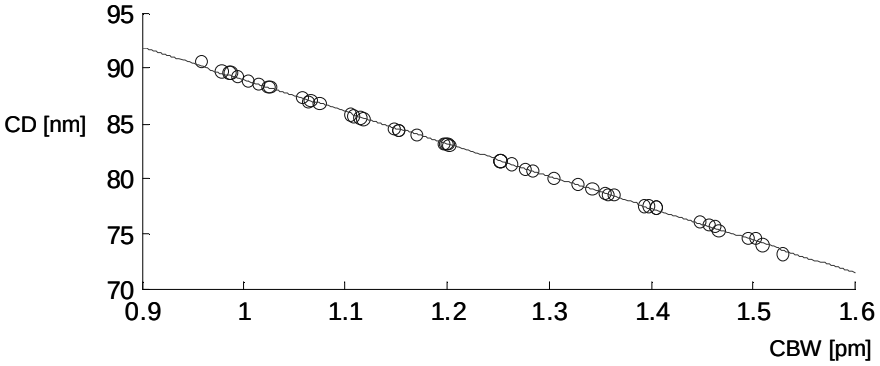

Figure 5. CD - CBW linearity

Although excellent correlation can be achieved with the CBW metric in this range of focus-drilling set-points, for focus drilling levels of 0.5pm to ~1pm, E95 based metrology and control may be preferred due to the diminishing sensitivity of the convolution based metric to changes in bandwidth caused by the characteristic width of the convolution function. The choice of metrology and control schemes based on the new spectrum measurement capability on board state-of-the-art light-sources will be dependent on the specific process application and will be described in a future publication.

2.4. Impacts of Higher-order Aberrations

So far in this work the process window and CD / proximity effect simulations assumed that the chromatic aberrations include only the longitudinal (chromatic defocus) term. Higher-order chromatic aberrations are typically ignored for lithography image calculation considering finite laser bandwidth.[6-11] Although this may be justifiable for nominal light-source bandwidths,[3,12] in this section we evaluate the imaging impacts of higher-order chromatic aberrations in focus drilling mode. The higher order chromatic aberrations Z5(λ) through Z37(λ) (where λ represents the wavelength dependency) for the ASML XT:1700Fi scanner were obtained experimentally and separately confirmed from design data. The simulation results show that the impact of the higher order aberration terms on DOF, EL and IPE are negligible for focus-drilling spectra up to 1.5pm E95. In Figure 6, we see that the difference in calculated DOF is less than 5% when higher-order chromatic aberrations are included compared to using the chromatic defocus term only; similarly the difference in EL is less than 4% and image placement error (IPE) changes by less than 0.2nm.

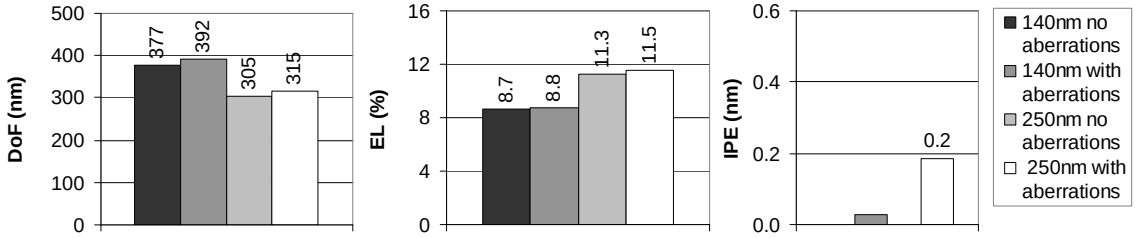

Figure 6. Impact of higher order aberrations on DOF, EL and IPE

The results shown here are for 72nm contact-hole patterns with 140nm and 250nm pitch, for spectra with 1.5pm E95. These simulations were carried out using 1.2NA and the soft annular illumination condition.

III. EXPERIMENTAL RESULTS

In this section we describe the results of wafer experiments validating the DOF enhancement by laser focus drilling. We also consider the impacts on CD uniformity (CDU), exposure latitude (EL), changes in optical proximity behavior and mask error enhancement factor (MEEF) using wafer exposures were obtained on an ASML XT:1700Fi / Cymer XLA™ 360 tool set. We also report on separate results of tool stability monitoring from a production ASML XT:1900Gi scanner in a fabrication facility on which a prototype Cymer XLR™ 560i laser focus drilling modules were installed and operated intermittently with nominal production operation.

3.1. Wafer Experimental Process Window, CDU and Overlay Results

In addition to quantifying the expected depth of focus performance enhancements for a specific patterning application, we experimentally investigate whether any of following side effects occur when switching from low to high bandwidth: (1) focus shift, (2) degradation of exposure latitude, (3) increase in CDU (4) changes in optical proximity behavior, (5) MEEF and (6) overlay, using a prototype laser focus drilling module. The focus drilling prototype was not actively controlled based on laser spectrum metrology feed-back as will be the case in the production version. The wafer exposures reported in this section where carried out on either the Cymer XLA™ 360 light-source and ASML XT:1700Fi or XLR™ 560i and XT:1900Gi with the following process conditions:

- The target CD is 85nm contact hole features, with CD tolerance +/- 10% for process window calculation. The mask targets for pitch in the range of 140nm to 385nm were manually selected for each setting to print at a target of 85nm with dose of 30mJ/cm^2
- In addition to the nominal laser bandwidth of 0.3pm E95, five focus drilling set-points were evaluated with E95 bandwidth of 0.8pm, 1.1pm, 1.2pm, 1.3pm and 1.35pm
- Two illumination conditions were considered: (1) 1.2 NA, with soft-annular 0.86 / 0.66 outer ring, 0.31 sigma and no polarization, and (2) 1.2 NA with annular 0.86 sigma outer and 0.66 inner ring, XY polarized

As expected, an appreciable improvement in depth of focus is observed for all laser focus drilling settings considered, as shown in Figure 7. These results are also compared with a scan-tilt based focus drilling technique, called EFESE™ Rx developed by ASML on its scanners for 500nm and 700nm focus range scan-tilt settings. In terms of focus range, the 500nm scan-tilt setting corresponds to approximately 1.1pm E95 for laser bandwidth and 700nm corresponds to approximately 1.35pm.

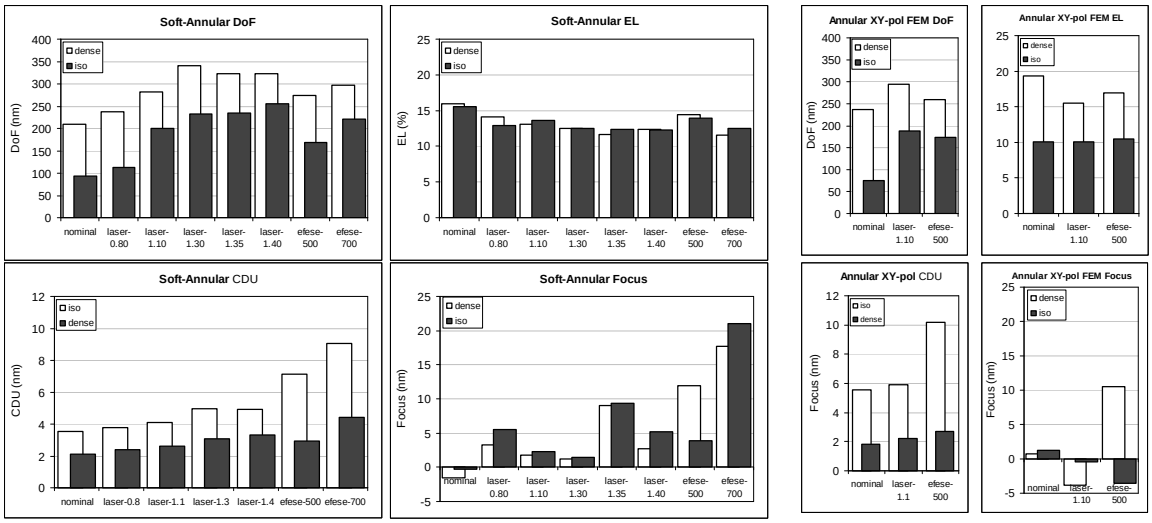

Figure 7. Changes in DOF, EL, CDU and Focus for an 85nm contact-hole process

The largest increase in DOF (62%) is obtained at the 1.3pm FD setting for the dense features with pitch of 140nm and the maximum DOF enhancement for most isolated features with 385nm pitch occurs at 1.4pm E95 (124%). Compared to the nominal laser bandwidth case (0.3pm E95) the corresponding penalty in exposure latitude is limited to 3.5% and 0.6% respectively. The maximum EL degradation through all laser focus drilling settings (0.3pm to 1.4pm E95), is limited to 4.3% for the conditions shown here. At the same time the CDU tradeoff is more severe and degrades by 1nm for dense features, which is still lower than the isolated contact CDU, which limits performance in this process; this may be an acceptable tradeoff if the process window is limited by the process window overlap, and particularly the DOF for isolated structures. The CDU reported here is obtained after removal of average field as well as the cross-wafer fingerprint leaving only the random contribution. Additionally, data in Figure 7 shows that the change in focus offset is well controlled, especially when compared with scan-tilt focus drilling. In table 1 we summarize the changes in process window metrics at the 1.3pm and 1.4pm laser focus-drilling setting for the isolated and dense contact structures.

It is interesting to note that using focus drilling values in excess of 1.1pm and 1.4pm E95 for annular XY-polarized and soft-annular illumination respectively do not result in a further increase in DOF. Beyond this, for the dense features a degradation of the DOF is observed while the EL and CDU remain roughly the same. Depending on the application, loss of image contrast limits the upper bound at which focus drilling can continue to produce an acceptable process window and an increasing DOF. For this data the 1-sigma reproducibility for the DoF and EL measurements is 9.8nm and 0.4% respectively.

	Soft-Annular	Soft-Annular	Soft-Annular	Ann-polarized	Ann-polarized	Ann-polarized
	DoF (nm)	EL (%)	CDU (nm)	DoF (nm)	EL (%)	CDU (nm)
dense (1.3pm)	62%	-3.5	-1.0	24%	-3.8	-0.4
iso (1.4pm)	124%	-0.6	-1.4	151%	-0.1	-0.4

Table 1. Process window metric changes at the 1.3pm FD setting for dense lines

The CD and proximity effect stability of the printed features over a 25-wafer lot was also verified. Figure 8 shows that CDU as well as IDB remain stable throughout the lot and are comparable to baseline system performance with nominal bandwidth of 0.3pm. The variability of CDU and IDB across a lot is <0.25nm.

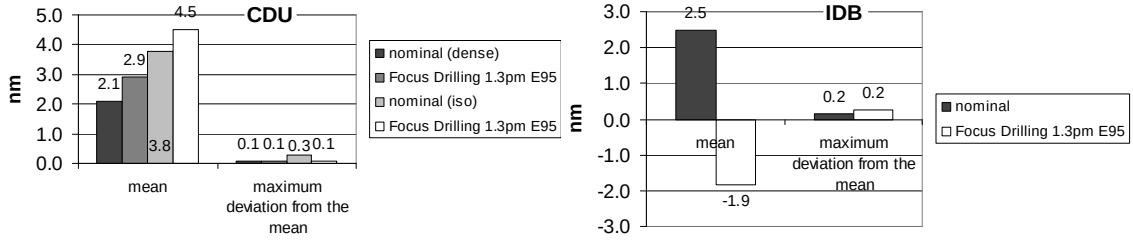

Figure 8. CDU and IDB variability through a lot of wafers

In previous work [12] it has been shown experimentally that the change in image placement error (IPE) from increased bandwidth settings of up to 0.5pm is very small, i.e. less than 0.5nm, for the same exposure tool type. Our simulations for higher-order aberrations described earlier in Section 3 also show negligible contribution to IPE. We have confirmed experimentally that the impact on overlay is quite small for levels of focus drilling up to 1.4pm. The data in Figure 9 shows an experimental result where the overlay error increases by 0.4nm when the 1st lithography layer is exposed using a nominal bandwidth setting of 0.3pm E95 (3.7nm) and 2nd layer exposed at a focus drilling set-point of 1.4pm E95 (4.1nm); both of these overlay exposures were carried out on the an XT:1900Gi / XLR 560i.

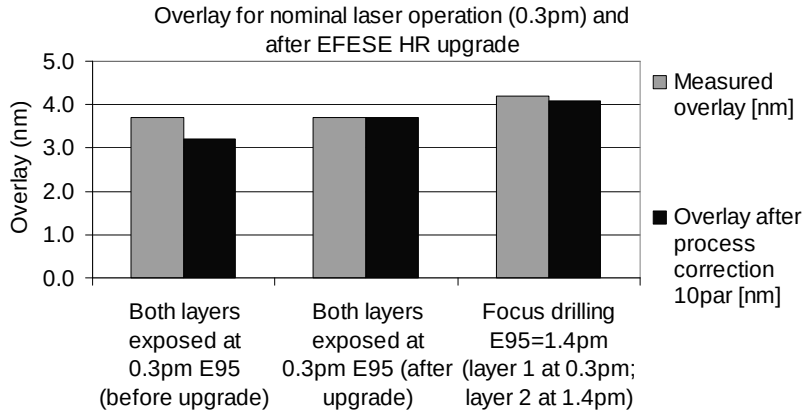

Figure 9. Overlay for nominal (0.3pm) laser operation and 1.4pm E95 focus drilling

Additional DOF data from XT:1900Gi / XLR 560i wafer exposures, using the unpolarized soft-annular illumination condition discussed previously are shown in figure 10. From this data we observe that laser focus drilling (EFESE™ HR) results in higher DOF and lower CDU compared to scan-tilt (EFESE™ Rx) across a range of focus drilling set-points. These experiments confirm our previous findings especially with regard to the CDU penalty related to scan-tilt (EFESE™ Rx) exposure.

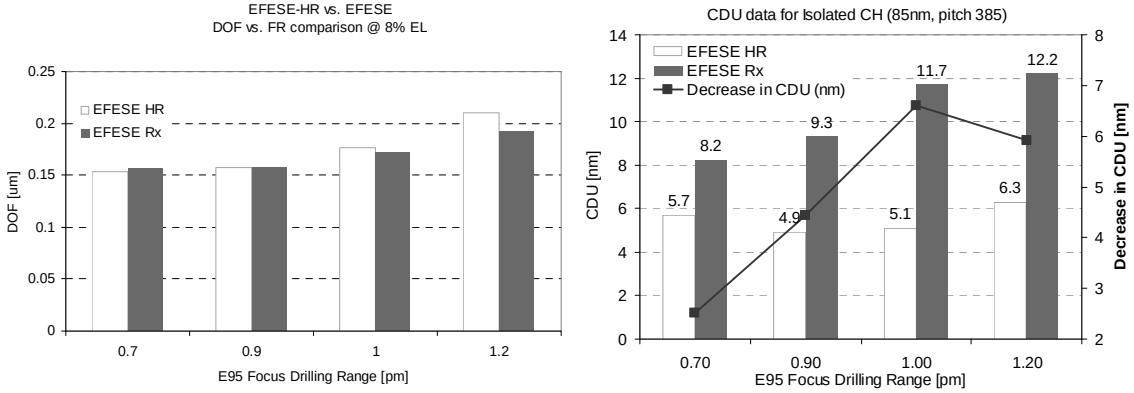

Figure 10. DOF and CDU at four laser FD (EFESE™ HR) and corresponding scan-tilt (EFESE™ Rx) settings

3.2 Optical Proximity Effects

In general the impact of laser FD on the optical proximity effect is similar to what has been reported previously as a function of changes in laser bandwidth [3,6,7,9,10] and the specific correction needs to be carried out to meet the CD targets for the desired application. In this work we investigated proximity curve changes when switching between the scan-tilt (EFESE™ Rx) and laser focus-drilling (EFESE™ HR) and we find that the behavior through-pitch for both methods can be matched to within 1nm, therefore requiring no additional change to the OPC. From data obtained at a customer site in Figure 11 we see that laser focus drilling can accurately match the scan-tilt (EFESE™ Rx) proximity behavior with maximum differences less than 1 nm, with the matching performed based on the CBW metric; this could potentially be reduced further by minor corrections to the illumination and / or focus-drilling set-point.

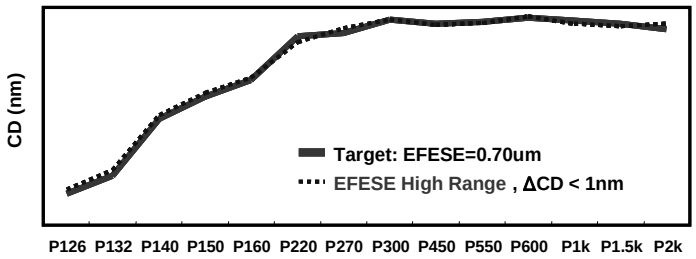

Figure 11. Proximity matching between scan-tilt (EFESE™ Rx) and laser focus drilling (EFESE™ HR)

For this example, the magnitude of the iso-dense bias (IDB) between nominal laser bandwidth and focus-drilling set-point of 1.3 pm E95 is less than 5nm, prior to correction, as shown in Figure 8. Additional data from the XT:1900Gi / XLR 560i optical-proximity matching experiments are shown in Figure 12 and confirm that proximity differences between focus drilling and scan-tilt EFESE™ Rx can be matched to less than 0.7nm using focus drilling bandwidth adjustment alone.

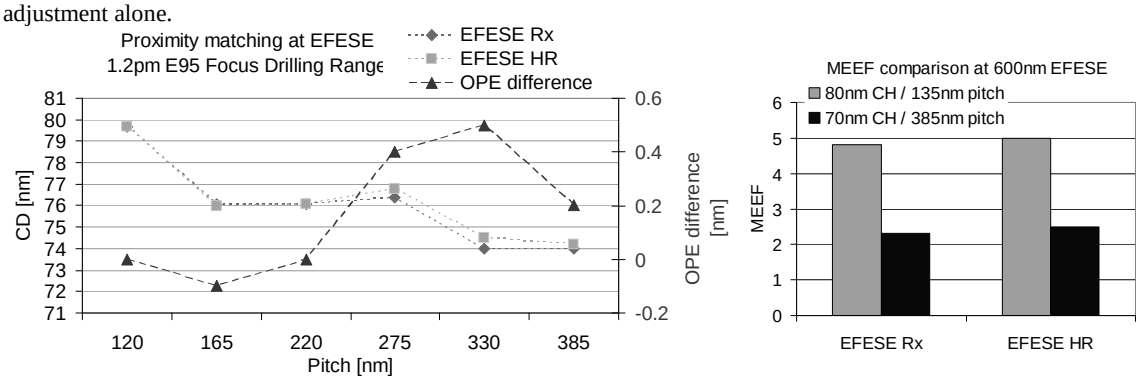

Figure 12. EFESE™ Rx and HR proximity matching (left) between and MEEF (right); XT 1900Gi wafer exposure

The plot on the right hand side of Figure 12 shows that there is no significant MEEF difference between scan-tilt at 600nm EFESE Rx setting and the equivalent laser focus drilling bandwidth of 1.2 pm E95. The change in MEEF between EFESE and laser FD is within the measurement accuracy.

3.3 Exposure Tool Stability Monitoring

In this section the results of exposure tool stability monitoring are discussed over one month of operation. A prototype laser focus drilling hardware was installed on a production tool at the customer site and performance was monitored over multiple weeks of operation. The prototype hardware did not include the new spectral metrology or feedback set-point control for focus drilling operation, discussed in section 2.2; therefore the monitoring data reflects open-loop stability performance. The data includes stability of best focus, depth of focus, image and aberration sensor performance. During the technology evaluation period, the lithography cluster was also operated in production mode with nominal light-source bandwidth operation, and stability of the system in nominal operation was equivalent to other systems of that type.

3.3.1 Best Focus Monitoring

Figure 13 shows the averaged best focus results using a customer's process wafer focus monitor collected over more than one month of system usage.

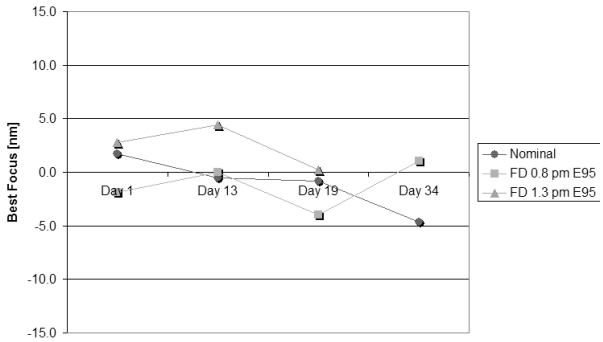

Figure 13. Best focus trend, chuck averaged

The wafer exposure uses a process-monitor mask and CD and wafer focus metrology is carried out using scatterometry. The focus stability over this period is +/- 5nm and we considered performance for two focus-drilling set-points of 0.8pm E95 and 1.3pm, which is generally within the experimental measurement noise. This performance is equivalent to variation for this process and equipment generation under nominal light-source operation as shown in Figure 13.

3.3.2. Monitoring stability of the process: Depth of Focus

The stability of the process window and DOF was also measured using the customer's Focus-Monitor test over three weeks of operation. For each monitoring data, the performance of two focus drilling set-points at 0.8 pm and 1.3 pm E95 were obtained and are compared with the nominal (non-focus-drilling) exposure. The DOF data are normalized to the baseline condition and are shown in figure 14; the data are in micrometers [μm] and represent a measurement which is highly sensitive to DOF changes. This data shows the observed increase in the DOF as detected from this wafer monitor for the two focus drilling settings and also very stable process performance over time. Again, this performance is obtained without closed-loop control for the laser focus-drilling set-point and with no compensation for spectral shape changes as discussed in sections 2.2 and 2.3. Additionally, on the right hand side in figure 14, the intra-wafer R^2 for the corresponding DOF data is reported, indicating stable across-wafer performance. It also shows that the stability at the highest focus-drilling set-point tested here (1.3 pm E95) is equivalent to nominal laser performance.

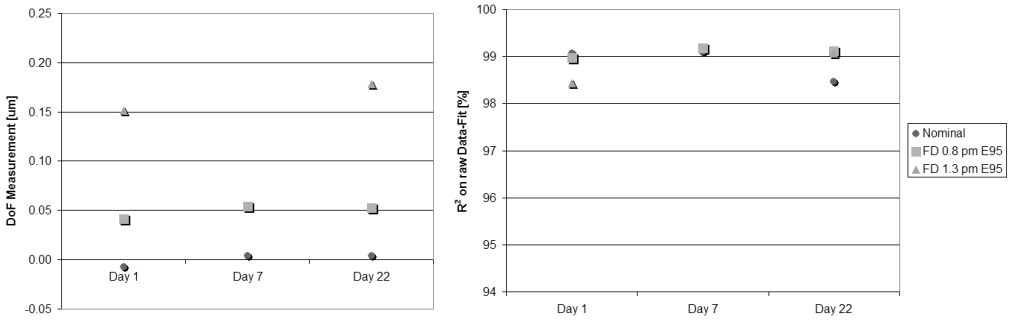

Figure 14. Normalized DoF measurement over time and R^2 from multiple points per wafer

3.3.3. Image Sensor Stability

The scanner image sensor measurement, shown in figure 15, were used to determine the image displacement errors in X, Y and Z direction and to quantify if the measurement reproducibility would be affected with the use of focus drilling. Over one month, transmission image sensor (TIS) measurements were performed on the ASML scanner at for the non-focus-drilling (nominal) condition as well as focus-drilling set-points of 0.8 and 1.3 pm E95.

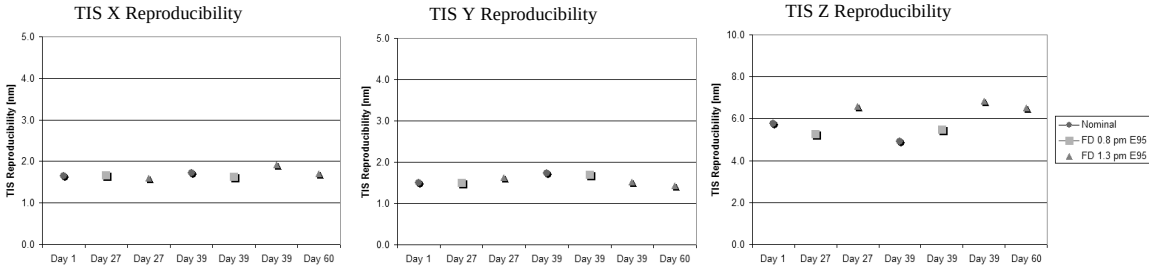

Figure 15. The maximum X, Y and Z image sensor repeatability measured by the exposure tool sensor

Although the Z data (focus) showed consistently higher reproducibility at the highest focus-drilling set-point (1.3 pm), the measured stability is very low and any changes are negligible. The same conclusion is reached for the lateral image position and the sensor reproducibility appears unaffected over the range of focus-drilling bandwidths and the period tested and reported here. Note again that the stability performance would even be expected to improve with additional closed-loop stabilization of focus-drilling set-point and compensation for spectral shape variation as determined using new spectrum metrology on the light-source as discussed in sections 2.2 and 2.3.

3.3.4. Aberration stability and repeatability

Scanner aberration sensor measurements were also carried out to determine if possible imaging or lens-manipulator changes would be observed at high levels of laser focus-drilling. It is also important to verify that the repeatability of the aberration sensor measurements do not degrade with the laser operating at high bandwidths in focus-drilling mode. The individual Zernike coefficient values (3sigma) for the Z5 through Z25 aberrations are shown in figure 16.

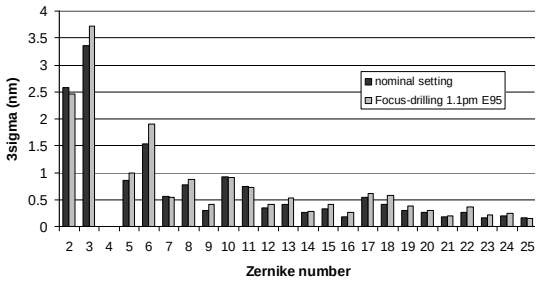

	nominal	1.1pm
z2-z25	1.73	1.73
z5-z25	0.90	0.99

Figure 16. Lens aberrations sensor measurement Zernike coefficients (left) and RMS data in table (right)

The average value is 0.9nm for the nominal case and 0.99nm for the high bandwidth case, which is acceptable performance. Additionally the aberration sensor measurement stability for laser focus-drilling operation is statistically equivalent to operation for nominal laser bandwidths.

IV. CONCLUSION

In his paper we present a laser focus drilling technique which has recently been developed for advanced immersion lithography scanners to increase the depth of focus and reduce process variability of contact-hole patterns. Focus drilling is enabled by operating the lithography light-source at an increased spectral bandwidth, and has been made possible by new actuators and metrology in advanced dual-chamber light-sources. We discussed wafer experimental and simulation results, demonstrating DOF increase by more than 50% with only a modest reduction in exposure latitude, contrast and CDU at best focus for 32nm logic and future technologies. Given the tradeoff engineering design, the optimum laser focus drilling set-point needs to be carefully defined to achieve the target depth of focus gain at an acceptable contrast, mask error enhancement factor and target optical proximity behavior. We show simulation results of the effects of higher-order chromatic aberration and show that image placement and critical dimension variation are minimally impacted for a range of focus drilling laser spectra. This paper points to the practical benefits of tradeoff design and co-optimization of the target focus drilling set-point and appropriately selected resolution enhancement approach to maximize the depth of focus and process-window overlap while increasing effectiveness of the source-mask solution for contact or via patterning.

ACKNOWLEDGMENTS:

The authors acknowledge the contribution of the following individuals in supporting the technology and product development, as well as valuable discussions and input to this manuscript. From Cymer this includes Rob Rafac, Daniel Brown, Rui Jiang, Raj Rao, Patrick O'Keeffe, Benjamin Lin and Kevin O'Brien, and from ASML, Herman Godfried, Laurens de Winter, Alena Andryzhyieuskaya, Jeroen Linders, Bart Smits, Marieke van Veen, Jasper Menger, Michel van Rooy, Sami Musa, Eric Verhoeven and Rob Willekers.

REFERENCES:

1. H. Fukuda et al., Improvement of defocus tolerance in a half-micron optical lithography by the focus latitude enhancement exposure method: Simulation and experiment, J. Vac. Sci. Technol. **B7** (4), 1989.
2. I. Lalovic et al., RELAX: Resolution Enhancement by Laser-spectrum Adjusted Exposure, Proc. SPIE Optical Microlithography XVIII **5754**, 447 (2005).
3. I. Lalovic et al., Illumination spectral width impacts on mask error enhancement factor and iso-dense bias in 0.6NA KrF imaging, Proc. BACUS XXI Photomask Technology Symposium **4562**, 112 (2001).
4. M. Terry et al, Behavior of lens aberrations as a function of wavelength on KrF and ArF lithography scanners, Proc. SPIE Optical Microlithography XIV **4346**, 15 (2001).
5. K. O'Brien et al., High-range laser light bandwidth measurement and tuning, to be presented at SPIE Optical Microlithography XXIV (2011).
6. K. Lai et al., Understanding chromatic aberration impacts on lithographic imaging, Journal of Microlithography, Microfabrication, and Microsystems (JM3), Vol. **2**, No. 2, pp 105-111 (2003).
7. J. Bakaert et al., Effect of laser bandwidth tuning on line/space and contact printing at 1.35 NA, *Proceedings of the 5th International Symposium on Immersion Lithography Extensions, The Hague, Netherlands, Sept 22nd – 25th, 2008.*
8. A. Kroyan et al., Effects of 95% integral vs. FWHM bandwidth specifications on lithographic imaging, *Proc. SPIE Optical Microlithography XIV* **4346**, 1244 (2001).
9. I. Lalovic et al., Defining a physically-accurate laser bandwdith input for optical proximity correction (OPC) and modeling, Proc. BACUS XXII Photomask Technology Symposium **7122** -62, (2008).
10. P. De Bisschop et al., Impact of finite laser bandwidth on the CD of L/S structures, Journal of Micro / Nanolithography, MEMS and MOEMS (JM3), Vol. **7**, No. 3, (2008)
11. M. Smith et al., Modeling and Performance Metrics for Longitudinal Chromatic Aberrations, Focus-drilling, and Z-noise; Exploring excimer laser pulse-spectra," Proc. SPIE Optical Microlithography XX **6520** -127 (2007)
12. U. Iessi et al., Laser bandwidth effect on overlay budget and imaging for the 45 nm and 32nm technology nodes with immersion lithography, Proc. SPIE Optical Microlithography XXIII **7640** (2010).

High-Range Laser Light Bandwidth Measurement and Tuning

Kevin O'Brien[1], Rui Jiang, Nora Han, Efrain Figueroa[*], Raj Rao, Robert J. Rafac
Cymer Inc., 17075 Thornmint Court, San Diego, CA, 92127, USA

ABSTRACT

High performance lithography is increasingly demanding light sources to deliver laser light over a much larger range of stabilized bandwidths. The applications range from improved optical proximity correction (OPC) to the high-speed printing of vias and contact holes, through a process called focus drilling. Several advances in light source technology must integrate to provide the improved bandwidth performance required by the industry.

This paper will outline three of the core technologies developed by Cymer and integrated into its most advanced XLA™ and XLR™ series light sources to meet this need. Novel improvements in line narrowing offer the actuation necessary to tune the bandwidth over the large range. Advanced bandwidth metrology yields accurate measurements of the bandwidth over the wide range. And new controls and feedback algorithms provide the integration to stabilize the bandwidth to the desired target. The result provides laser light bandwidths that can be tuned to and accurately stabilized at any spectral E95 target from 0.3 pm to 1.6 pm, while maintaining all other laser performance parameters. The feature is called focus drilling. Focus drilling extends the utility of Cymer XLA and XLR lasers by adding more flexibility to the light source, allowing the end-user chipmaker to select the exact properties of the laser light necessary for a wider range of process steps.

The article will discuss the above technologies and emphasize their important aspects. It will also highlight some of the key performance aspects using data from Cymer's testing. Some of the design features and trade-offs will be provided, and a few of the relevant metrics will be presented and justified. Finally, potential future improvements to the technology will be presented.

Keywords: laser, bandwidth, focus drilling, laser metrology

[1] kobrien@cymer.com, phone: int+1-858-385 6315, www.cymer.com
[*] Now an independent agent, no longer with Cymer, Inc.

1. INTRODUCTION

Advanced lithography systems are offering rapidly increasing performance in response to market demands. Among these performance improvements are better reliability, increased availability, and higher throughput. Throughput is increased through many means, including via the laser light source. To help increase throughput, the laser can provide tighter stability of light properties, such as better dose stability; new features, such as bandwidth tunability; or a wider range of operational capability, such as higher power. Cymer has developed these and other important improvements throughout its history.

Cymer is continuing to improve its XLA and XLR series DUV light sources by developing the capability to operate over and tune to a much wider range of laser light bandwidths. Such capability can be applied to, for example, a focus drilling system, where very high bandwidths can reduce loss of focus latitude when printing features such as contact holes and vias (see Reference [1]), while maintaining process stability. While methods to significantly increase bandwidth range have been proposed in the past (see Reference [2]), the demonstrated maturity of the technology described in this paper allows a robust, stable, and seamless solution. This new technology is currently deployed at a high volume chipmaker.

The higher bandwidths are achieved mostly by a new line narrowing module (LNM) with an advanced bandwidth actuation mechanism. However, to properly stabilize and report the higher bandwidths, fundamentally new bandwidth metrology is required, and a new control scheme is needed to integrate these. These three key elements are described, with emphasis on capability and important technological aspects. Some Cymer test data is given showing examples of the new capability, and some trade-offs will be discussed. Finally, potential enhancements to the technology are offered.

2. LINE NARROWING IMPROVEMENTS

Cymer developed the new focus drilling LNM to provide the significantly wider laser light spectra and the ability to rapidly change it from narrow to broad. It is coupled with the existing Cymer Active Bandwidth Stabilization™ (ABS™) technology to provide a dual stage actuation of bandwidth (see Reference [3]). This allows existing ABS laser systems to perfectly retain their existing low bandwidth performance, while adding the high bandwidth capability as an upgrade. The new LNM fits within the existing LNM location in the laser, and requires only minimal additional hardware and connections to enable it. All of these features imply the high-range bandwidth system adds the new capability seamlessly, with minimal upgrade downtime, and without compromising existing performance.

The maximum bandwidth with the new LNM, as measured by spectral E95[2] (hereafter called simply E95), is increased to over 1.6 pm from a prior typical maximum of 0.5 pm. A recently introduced bandwidth metric, called Convolved Bandwidth (CBW)[3], can also be increased to over 1.5 pm. Figure 1 shows these metrics against the new actuation in the LNM. Note that the existing ABS bandwidth actuation range is maintained, able to achieve up to 0.5 pm. Importantly, with this actuation scheme, the spectrum is broadened with very little impact to other laser operational parameters such as wavelength stability and energy stability.

The speed of the new actuation is also an important performance metric, as it defines the stabilization and switching capability of the final closed loop system. The actuation responds as a first order asymptotic, with a time constant of 650 milliseconds, delay of less than 50 ms, and highly symmetric response with no hysteresis[4]. Figure 2 shows some step responses.

---

[2] Spectral E95 is the standard bandwidth metric among immersion systems.

[3] CBW is basically a measure of the laser spectrum's "appearance" to the optical system of the scanner. It will be discussed in more detail in Section 3.

[4] The CBW response may appear to have longer delay and be slower in the negative direction; this is due to the CBW's insensitivity to actuation at low values, and not actuation speed. A compensation method is described subsequently.

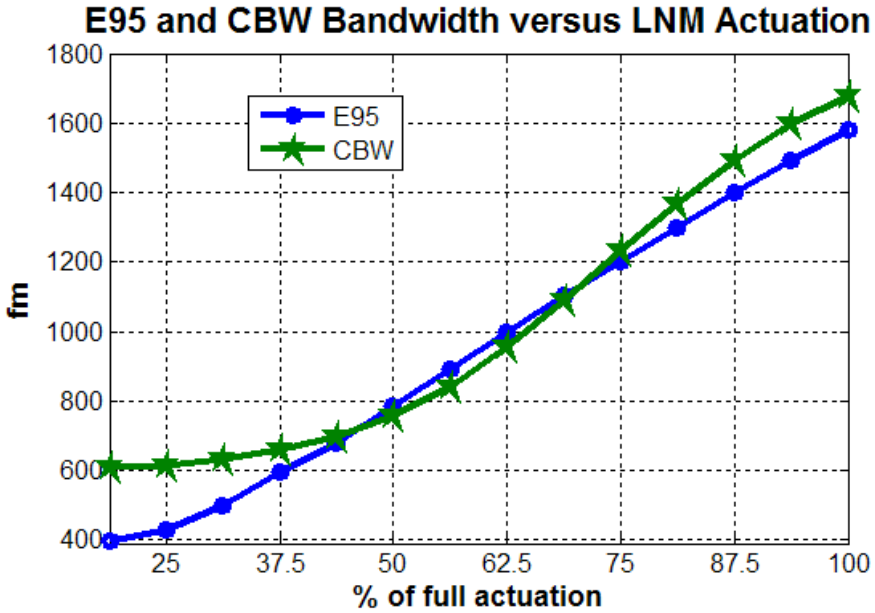

Figure 1. Bandwidth versus actuation, showing large nonlinearity of CBW

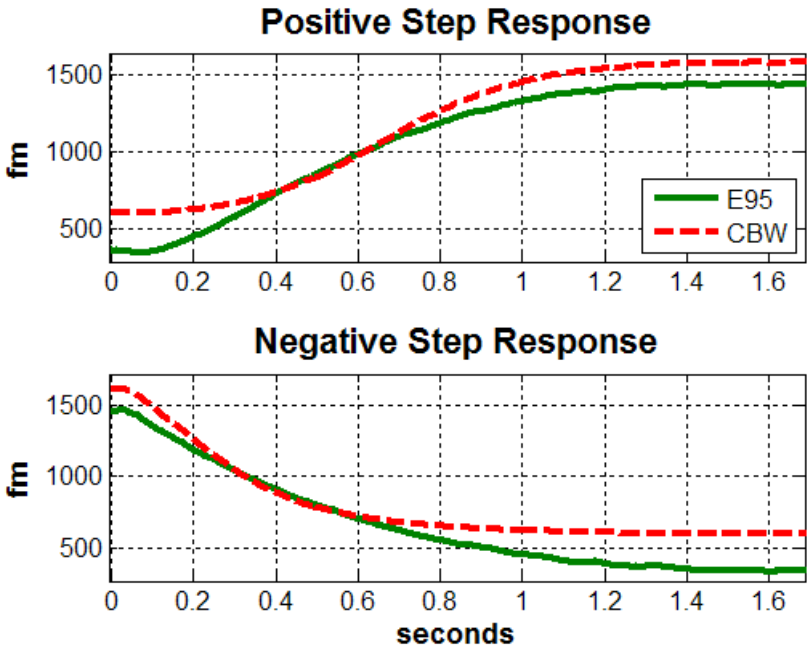

Figure 2. Bandwidth actuation speed of response

3. ADVANCED BANDWIDTH METROLOGY

A bandwidth metrology that accurately measures the laser's spectrum over the very wide range provided by the new actuation mechanism discussed in section 2 was required. It must be capable of measuring not only the standard metrics of E95 and Full Width at Half Maximum (FWHM), but also the spectral shape, with the introduction of the new CBW metric. Moreover, it needs to perform these tasks at a high rate sufficient to report on a burst-by-burst basis.

Figure 3 shows the bandwidth metrology process steps. The etalon fringe data is first pre-processed by an algorithm that continually estimates and compensates for the image sensor reference changes and error sources to minimize effects from limited mechanical tolerances and thermal drift. The new bandwidth metrology then recovers an estimate of the spectrum that is optimal in the least-squares sense, by using advanced proprietary signal processing on the pre-processed and prepared sensor data and calibration factors. The post-processor filters in both the sample and spectral domains to minimize de-convolution process noise (e.g. Gibbs oscillations) and speckle effects. All these processes are combined and tuned in unison to yield the optimal spectrum estimate, which is the most accurate given the system characteristics. Figure 3 shows the process steps graphically.

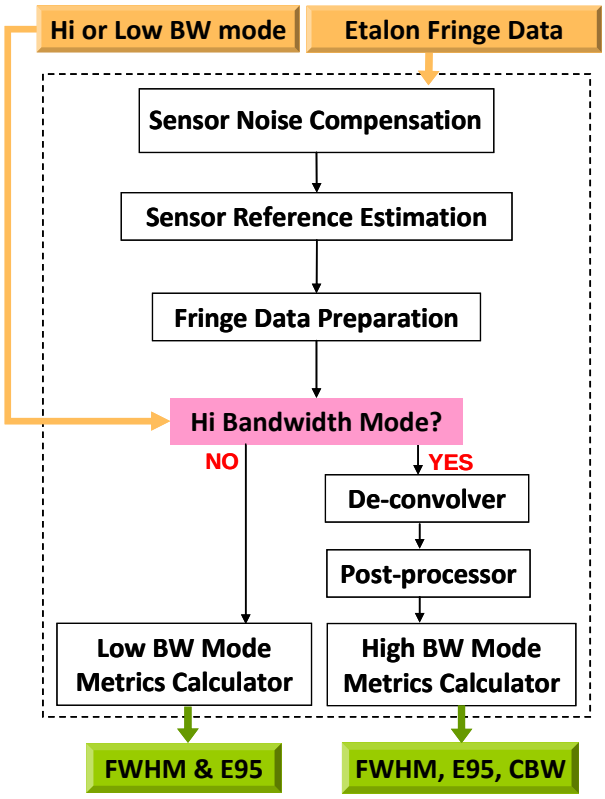

Figure 3. Bandwidth metrology process

There are some trade-offs. Filtering can reduce, but not eliminate, noise and speckle effects. Longer sensor exposures, which tend to average noise and speckle, often yield a more accurate measurement. Longer exposures, however, come at the cost of reduced reporting frequency. This trade-off effectively places a bound of spectrum measurement accuracy for a given reporting rate. The new metrology can be adjusted to operate anywhere within this trade space: from longer-exposures and better accuracy, to shorter exposures with less accuracy. The parameters are tuned to yield performance very near the accuracy bound for the chosen regime. For a reporting rate of once per burst, the accuracy is shown in Figure 4.

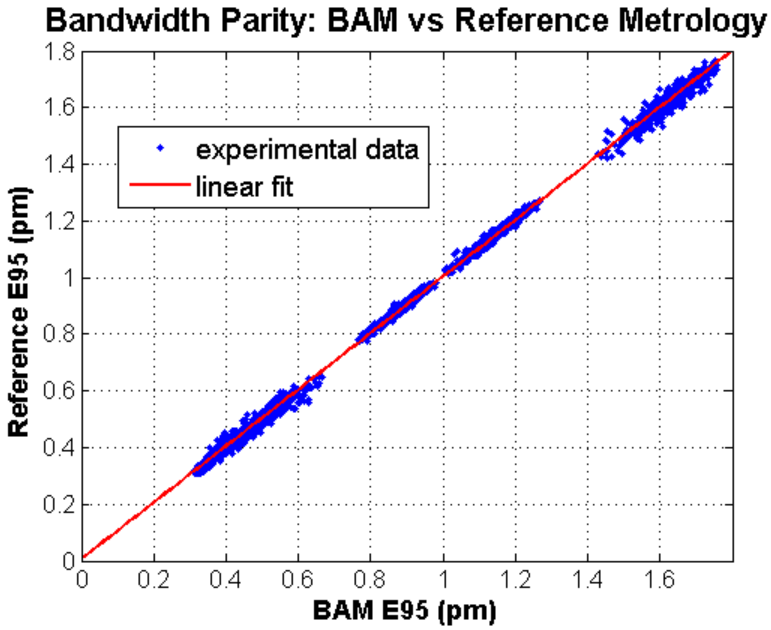

Figure 4. Parity of new metrology versus reference metrology

As with the new LNM, the new bandwidth metrology module (BAM) also operates identically under the normal low bandwidth modes as existing metrology modules, as shown in Figure 3 (see also Reference [4]). This allows the system in low bandwidth mode to perform the same after the upgrade as before, minimizing disruptions and process variations. The metrology switches between the low and high bandwidth modes smoothly and quickly when the system requires it. The system is calibrated to provide maximum accuracy in both modes.

The new CBW metric is computed in the new metrology. It is the FWHM value of a convolved spectrum obtained by convolving the laser spectrum with an "image function", representing the spectral response of some part of the system receiving the light. Note that such a convolved spectrum is the actual effect of the laser spectrum on this part of the system. Figure 5 shows the process graphically.

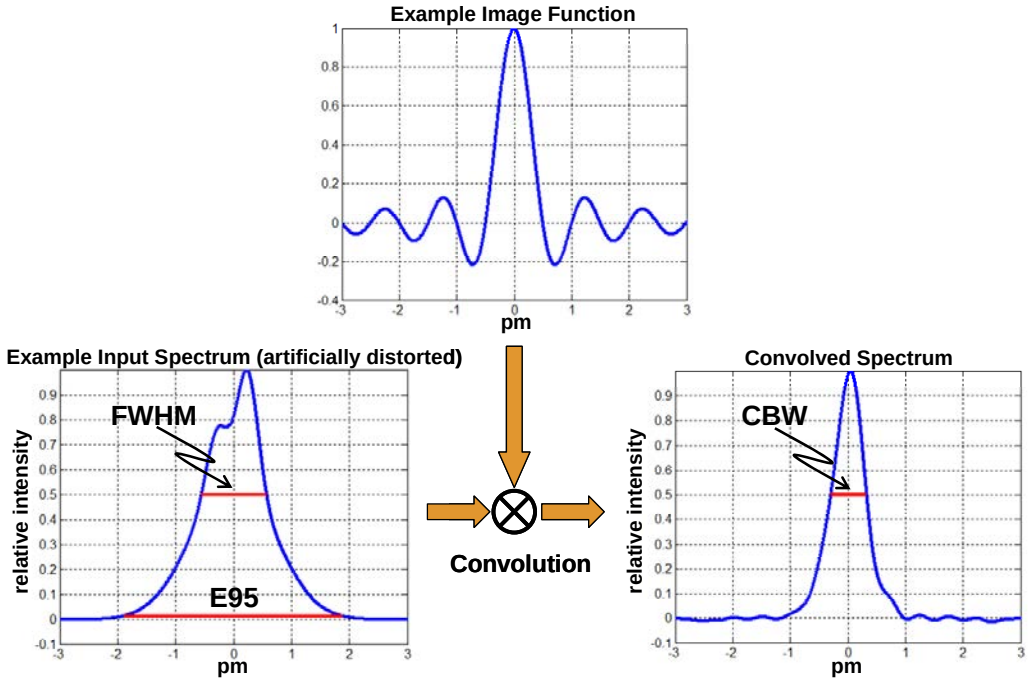

Figure 5. Computation of convolved spectrum and CBW

4. NEW CONTROLS AND INTEGRATION

The new hardware technologies discussed in the previous sections require integration and control to achieve and maintain specified bandwidth performance. Two key performance metrics are bandwidth stability (or disturbance rejection) and time to switch between low and high bandwidth operation. Each of these is enabled through several new controls technologies, some acting together and others acting independently. The system may operate in two modes to coincide with the metrology's modes: low bandwidth and high bandwidth. Within these modes, the target bandwidth can be selected to any value within the system's operating range.

When the system is operating in low bandwidth mode, stability as achieved exactly as existing technologies (see Reference [3]), which eliminates performance variations and disruptions when upgrading to this new technology. When the system is operating in high bandwidth mode, bandwidth stability is achieved through both closed and open loop control. The closed loop uses the new bandwidth metrology as the feedback sensor, the new line narrowing as the actuation, and advanced high-performance feedback and feed-forward algorithms to control and integrate these. Figure 6 shows the control system architecture. The system is capable of controlling E95 or CBW based on user commands. The feedback algorithm uses integral feedback with compensation for resulting phase lag and intergrator wind-up. The feed-forward algorithm works by estimating the bandwidth-versus-actuation gain and inverting it. The estimation is based on both the current actuation command and knowledge of Figure 1. Therefore, depending on whether E95 or CBW is being controlled, the feed-forward algorithm selects the appropriate gain. This reduces design and implementation complexity by allowing the feedback algorithm to remain unchanged between E95 and CBW control, since the loop will always be tuned as system whose bandwidth-versus-actuation gain is near unity. Performance of this closed loop, compared to open loop, is shown in Figure 7, demonstrating the rapid convergence to large artificially induced step disturbances and large attenuation of a large artificially induced sinusoid disturbance.

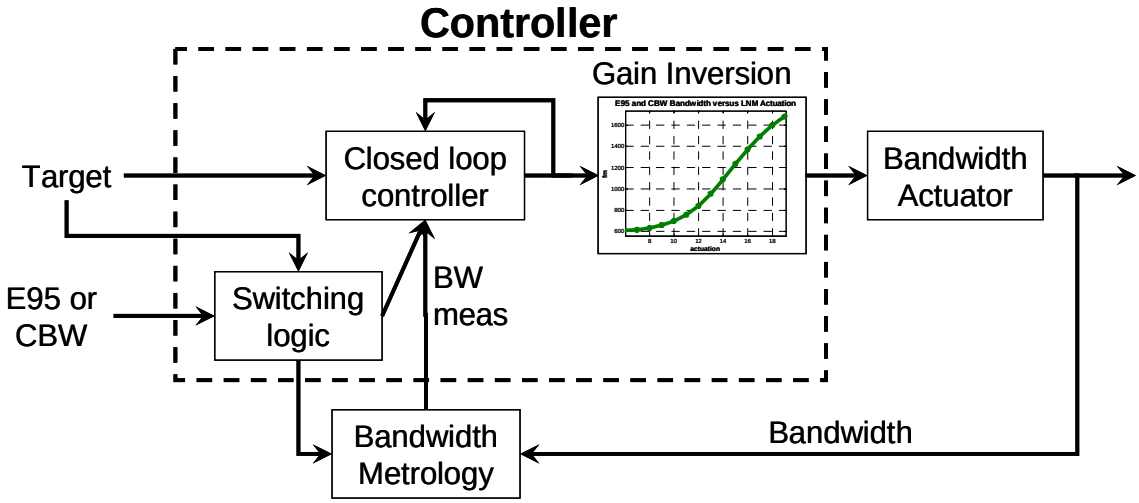

Figure 6. Bandwidth controller architecture

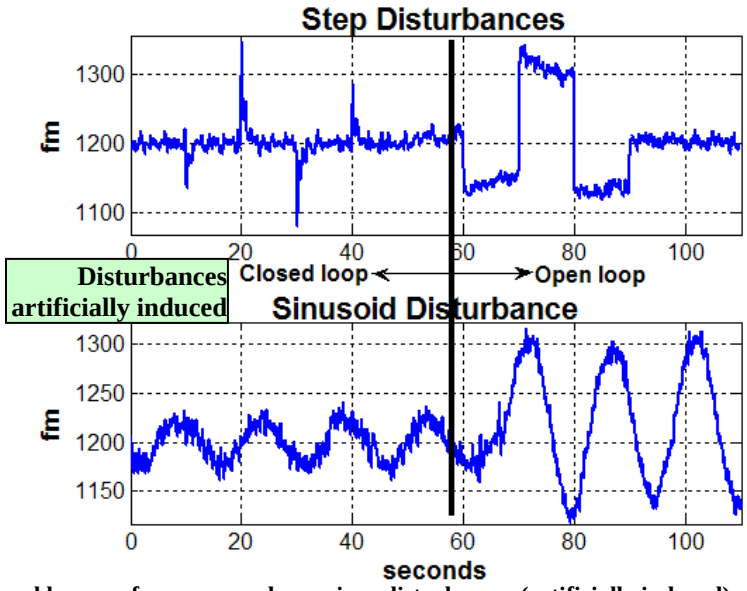

Figure 7. Closed loop performance under various disturbances (artificially induced); compare to open loop.

As mentioned, the target bandwidth can be changed at any time to any operational value. To maximize the speed when switching between different bandwidth targets, the controller uses a pre-drive mechanism and knowledge of Figure 1 to effectively select the LNM actuation needed for any new target. The closed loop removes any residual error. The performance of this switching scheme is shown in Figure 8. Comparing this to the step responses in Figure 2 shows the closed loop switching achieves nearly maximum possible performance. Additionally, if the system operates for an extended period (several days or weeks) in high bandwidth mode before returning to low bandwidth mode, measurable drift in performance can occur in the low bandwidth mode. To counteract this effect, a secondary closed loop, using the original ABS actuation and sensing, is used to assure that the bandwidth in low bandwidth mode is restored to the desired target.

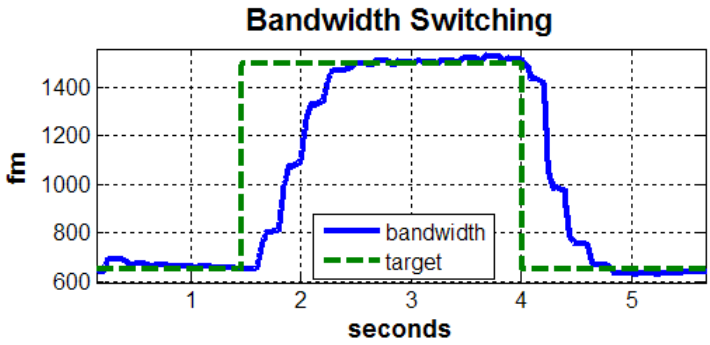

Figure 8. Bandwidth switching performance.

Large changes in bandwidth have the potential to disturb the laser's efficiency. Because well regulated efficiency is so important to the lithography scanners, the control system also includes several components to assure efficiency changes are managed and controlled. The system will observe any changes in efficiency, adapt to them quickly, and restore normal operation all within the time required to change the bandwidth to a new target.

Finally, the new controller manages the new metrology module by commanding it to switch to the desired mode (low or high bandwidth) at the appropriate times, and by maximizing use of the available data. For example, the low bandwidth mode metrology provides a fully updated bandwidth reading more frequently than the high bandwidth mode. The controller can then be made faster in this mode.

5. BANDWIDTH CONTROL POTENTIAL ENHANCEMENTS

As the lithography industry continues to evolve and progress, it is expected that tighter bandwidth stability, and more rapid bandwidth tuning will be required to maintain and increase throughput. The technology described in this paper can be enhanced in a relatively straightforward fashion to yield all of these improvements. Faster tuning can be accomplished through larger actuation hardware, or slight modifications of the hardware design. Tighter bandwidth stability is a matter of more advanced control algorithms that can observe and manage, in real-time, some of the nonlinear or transient effects of the bandwidth. Better stability can also be achieved through more fundamental means of control, such as laser alignments and tuning or by adding finer and faster actuation mechanisms.

6. CONCLUSIONS

Higher range laser light bandwidth can provide a significant jump in lithographic process capability and performance, improving focus latitude without loss of throughput, used when printing some specific features such as contact holes and vias. Cymer has introduced a new technology to provide a robust, switchable, and tunable high range bandwidth solution on its XLA and XLR series advanced laser light sources. New actuation mechanisms, advanced metrology, and tightly integrating controllers combine to yield the desired performance, which has been demonstrated in this paper, and at a large high volume chipmaker.

The technology is also robust, easy to upgrade, and does not disrupt or change any existing performance characteristics, even across the upgrade, ensuring continuous and seamless lithography cell operation. As the demands on bandwidth tuning continue to increase, this technology can be scaled well to meet these demands. It represents an added flexibility of Cymer light sources to the lithography manufacturer.

7. REFERENCES

[1] Lalovic, I., Lee, J., Seong, N., Farrar, N., Kupers, M., van der Laan, H., van der Hoeff, T., Kohler, C., "Focus Drilling for Increased Process Latitude in High-NA Immersion Lithography", *Optical Microlithography XXIV*, Proc. of the SPIE 2011, to be presented.

[2] Lalovic, I., Farrar, N., et al, "RELAX: Resolution Enhancement by Laser-spectrum Adjusted Exposure", *Optical Microlithography VXIII*, edited by Bruce W. Smith, Proc. of SPIE Vol 5754, 2005

[3] Brown, D.J.W., O'Keeffe, P., Fleurov, V.B., Rokitski, R., Bergstedt, R., Fomenkov, I.V., O'Brien, K., Farrar, N.R., Partlo, W.N., "XLR 500i: Recirculating Ring ArF Light Source for Immersion Lithography", *Optical Microlithography XX*, edited by Donis G. Flagello, Proc. of SPIE Vol 6520, 2007.

[4] Rafac, R. J.,, "Overcoming limitations of etalon spectrometers used for spectral metrology of DUV excimer light sources", *Optical Microlithography XVII*, edited by Bruce W. Smith, Proc. of SPIE Vol. 5377, 2004